Dynamic evaluation of airflow stream generated by a reverse system of an axial fan sprayer using 3D-ultrasonic anemometers. Effect of canopy structure

Ramón Salcedo, Pau Pons, Jordi Llop, Tomás. Zaragoza, Javier Campos, Paula Ortega, Montserrat Gallart, Emilio Gil*

Department of Agri-Food Engineering and Biotechnology, Universitat Politècnica de Catalunya, Esteve Terradas 8, Campus del Baix Llobregat D4, 08860 Castelldefels, Barcelona (Spain).

[*]**Corresponding Author:** Emilio Gil, DEAB, Universitat Politècnica de Catalunya, Esteve Terradas 8, Campus del Baix Llobregat D4, 08860 Castelldefels, Barcelona (Spain).

Tel: +34 93 552 10 99; Fax: +34 93 552 21 001

E-mail: emilio.gil@upc.edu

Website: https://uma.deab.upc.edu/en

Abstract

Air assisted sprayers are currently used for the applications of plant protection products in fruit trees and vineyards. However, the use of these equipment carries a high environmental risk, mainly owing to the generation of airborne spray drift in the lower boundary layer above crop canopy. Hence, many tests are currently focused on investigating several factors that affect the efficiency of the spray process, in which air assistance and air behaviour are two of the most difficult parameters to evaluate. This present work proposes a first approach on the characterization of the airflow generated by an orchard sprayer equipped with an axial fan and an air reverse system in the outlet plane of the air, while circulated through two artificial rows of canopy representing vineyard trellis, using 3D-ultrasonic anemometers to measure the experimental data. A first series of static field tests measured the air velocity at different heights on both sides of the sprayer and at both sides of every row of artificial canopy and evaluated the effect of the canopy on the sprayer airflow passing through. A second set of experiments were carried out with the sprayer moving at 4.1 km h^{-1} between canopy rows to simulate the normal spray process. Finally, velocity vectors and turbulent intensities were calculated. The resistance of the vegetation was also characterized by using a drag coefficient, both when the sprayer was stationary and moving. The results between the static and dynamic tests were compared. Although there were similarities between the two tests, the results indicated that when the equipment moves along the canopy rows, the axial fan asymmetry on air velocities is more noticeable and turbulence intensity increased. In addition, the vegetation received direct airflow at different times. This could affect the trajectory of the droplets. On the other hand, the resistance of the vegetation on each side was similar. The air reverse system could be affecting the airflow direction to the driving direction. Ultrasonic anemometers were successful in characterizing sprayer fan airflows but it is necessary to continue working on the descriptive analysis of the airflow in other planes different from the air outlet only and with other vineyard systems.

Keywords

Air assisted sprayers; outlet plane; artificial vineyard; Static and dynamic assays; Velocity profile

Funding

This research did not receive any specific grant from funding agencies in the public, commercial, or not-for-profit sectors.

1. Introduction

Disease control and the use of pesticides in crop cultivation is a critical issue in the agricultural sector (Damalas, 2015). Crop treatment with pesticides can be a risk not only to the environment (Carvalho, 2017), but to humans as well (Mamane *et al*., 2015); further, is one of the most important economic factors for a farmer (Ganesh, 2018). Hence, pesticide spray applications offering reduced costs and improved efficiency, have been empirically developed over the decades (Das *et al*., 2015).

In the case of tree crops and vineyards, farmers use sprayers equipped with different air-assistance systems, such as crossflow, individual spouts or axial-flow fans (Dekeyser *et al*., 2011). The use of air-assisted sprayer has advantages that help optimize the treatments (Moltó *et al*., 2006): it is required only the driver of the tractor, working time is short enough to act at the time of greatest sensitivity of the pest or these machines imply a more rational use of water consumption and chemical products. These sprayers generate airflow helping the transport and penetration of pesticide droplets to be directed into the vegetation in uniform distribution (Walklate *et al*., 1996, Panneton 2005ab). This mechanism focuses the applied volume to the vegetation target diminishing unwanted losses and improving the efficiency of the treatment.

But not all the product reaches the target vegetation. The airflow also sends a fraction of the applied volume into the air (Gil and Sinfort, 2005). This fraction of product carried out of the target area by the action of the environmental wind is defined by ISO Standard

22866 (2005) as a spray drift. This phenomenon not only reduces the efficiency of the treatment (Landers, 2008) but also endangers the environment (Garcerá *et al*., 2017), as pesticide droplets maybe carried by environmental air currents to sensitive areas such as populated areas (Butler-Ellis *et al*., 2017) or water resources (Ochoa and Maestroni, 2018). This brings the necessity to consider airborne spray drift in air-assisted pesticide sprayers (Kasner *et al*., 2018). The control of spray drift is the first environmental problem during the design of air-assisted sprayers and their use (Fornasiero *et al*., 2017; Grella *et al*., 2019).

Therefore, airflow behaviour is a key element on the efficiency of pesticide treatments with air-assisted sprayer. In this way, most research focus on the analysis of airflow influence, such as in spray distribution (Pergher and Gubiani, 1995; Cross *et al*., 2003; Farooq and Landers, 2004; Balsari *et al*., 2008; Pergher and Petris, 2008; Celen *et al*., 2009; Miranda *et al*., 2015, 2017; García-Ramos *et al*., 2018) or the droplet size (Reichard *et al*., 1977 and 1992; Cross *et al*., 2001; Czaczyk, 2012; Miranda *et al*., 2018; Balsari *et al*., 2019). Moreover, most of the above studies do not include a physical description of air behaviour. This is important because knowing how air is produced by the sprayers simplifies the understanding of the whole phenomenon— starting from the droplets leaving the nozzles –taking into account the type of sprayer, the air system design, the air inlet conditions, the asymmetry of the air system, the forward speed and the natural air currents and the artificial airflow–, until they reach the vegetation, in which they may penetrate the canopy, pass through the canopy or rise above the vegetation and be affected by the natural wind that drifts them into the surrounding air. That is why its study is considered a fundamental need for improving the efficiency of treatments with this type of machines (Zhai *et al*., 2018).

The sprayer design will determine the behaviour of the outgoing airflow (Triloff 2016; Van de Zande *et al*., 2017). The number, shape and size of the outlets, the air system employed and the amount of spray volume influence the efficiency of the treatment (Pezzi and Rondelli, 2000; Walklate and Richardson, 2000; Cross *et al*., 2003; Chen *et al*., 2013; Duga *et al*., 2015). Currently, farmers use crossflow fan sprayers or with individual spouts that are adapted to the characteristics of the crop. There are also research groups working on an adjustable air equipment (Hołownicki *et al*., 2017; Longlong *et al*., 2017). Nevertheless, the traditional equipment is the air blast sprayers with an axial fan (Fox *et al*., 2006), as it allows to apply pesticides with large airflow volume rates. In these sprayers, the fan design (Cross *et al*., 2003), its fan speed (Wei *et al*., 2016), and the inclusion of deflectors (Celen, 2008) influence the airflows that carry the droplets to the target.

During the generation of airflow, there are differences in the magnitude and direction of the air velocity vectors between both sides of the sprayer. Theoretically, manufacturers design the sprayers to reduce this asymmetry to ensure that the droplets reach the vegetation in a similar way on both sides. Following this assumption, several researchers analysed only one side of the fan (Delele *et al*., 2005; Da Silva *et al*., 2006; Endalew *et al*., 2010b; Duga *et al*., 2015; Salcedo *et al*., 2015). However, these differences depend of other factors, such as the forward speed of the equipment, and could become more larger, affecting the trajectory of the droplets to the target vegetation.

The movement of the sprayer causes deflection on the fan airflow (Ghosh and Hunt, 1998). The forward speed of the equipment modifies the air currents around tractor and sprayer, thus causing changes in airflow direction of the fan and magnitude (Reichard *et al*., 1979) that can affect the transportation of droplets.

These previous factors influence the stability of the airflow during the treatment. Brazee *et al*., (1981) analysed the turbulent mechanics produced during the spray applications with air blast sprayers. This turbomachine generates an airflow with a high variation of the velocities, including effects of diffusion, mixing and dissipation. It could also normalize the concentration and trajectories of pesticide droplets in the air (Delele *et al*., 2005, 2007). This variation could be enhanced by the presence and interaction of airflows with the vegetation (Walklate *et al*., 1996, Świechowski *et al*., 2004; Panneton 2005ab). The effect of vegetation on the air also needs to be studied in depth (Li *et al*., 2018). Interaction between the airflow coming from the fan and the vegetation generates modifications and turbulences inside the vegetation and around the canopy (Finnigan, 2000; Finnigan *et al*., 2009). The vegetal mass absorbs the kinetic energy of the air, producing losses in velocity and pressure (Belcher *et al*., 2003), which could produce deviations on the droplet trajectory and ability to penetrate into the canopy. The intensity of this interaction will depend on the vegetal characteristics. In this case, the type of tree crop or vineyard is very important, because the size and density of the vegetation vary in each case. Hence, Da Silva *et al*. (2006) presented a methodology to determine a drag coefficient that characterizes the aerodynamic resistance in vineyards, but that could be extrapolated to more tree crops, such as citrus (Larbi and Salyani, 2012a, 2012b) or pear trees (Endalew *et al*., 2010a, 2010b). Furthermore, the shape and density of the vegetation should also be considered, as variations in this parameter can generate different turbulent structures or vortexes canopies around the canopy (Salcedo *et al*., 2015), which increase the instability of the airflow around the vegetation and expose more droplets to the natural air currents.

These factors have become more important because many farmers wish to use their sprayers at high forward speeds. In this situation, the trees itself and the airflow inside the vegetation forms an obstacle when the sprayer is moving. The velocity of the airflow arriving to the vegetation reduces by increasing forward speed (Delele *et al*., 2005; Triloff, 2011). This is because when the forward speed is increasing then airflow direction is more oriented to the back part of the sprayer. In addition, when the airflow penetrates the vegetation the velocity decays as faster as the forward speed increases (Walklate *et al*., 1996). In this way, if the vegetal density is very high, the airflow cannot penetrate the canopy and go to the lower boundary layer of air (Salcedo *et al*., 2015). All this can influence on the spray deposition in the vegetation (Triloff, 2015, 2016 and 2018). For this reason, a description of the vectors of the air flow is necessary to understand what happens in that moment and to adjust the design of future fans.

Because most studies at present deal with static airflow, it is important to study the dynamics of the airflow from a forward moving sprayer. The main problem for the dynamic assays is the high complexity owing to the large number of variables involved, and the difficulty to include or analyse them during the displacement of the sprayer. De Moor *et al*. (2002) confirmed that there is a relationship between the airflows characterized during static and dynamic experiments. However, De Moor *et al*. (2002) did not include the vegetation effect on the airflow nor a characterization using velocity vectors. García-Ramos *et al*. (2012) did not include these variables in their analysis of the airflow of a sprayer equipped with two fans either. Gu *et al*. (2012) measured the air jet velocities from an air assisted five-port sprayer in an open field without obstacles. Endalew *et al*. (2010b) experimented with different sprayers but with the main objective to achieve experimental data to design computational fluid dynamics (CFD) models.

In addition, all air assays should take into account the methodology, such as the number or distance between measurement points, and the anemometer. There are different types of sensors used in the literature. The propeller anemometers are simple and easy to use but they do not offer information about the direction of the flow. Moreover, these sensors run on the peaks of the airflow velocities and need a long sample time. Hot wire anemometers and Pitot tubes give information about the velocity magnitude in each component. These sensors are very useful for calculating the airflow rate or studying the airflow that passes through a unidirectional conduit and areas close to the air outlet (De Moor *et al*., 2002; Cross *et al*., 2003; Świechowski *et al*., 2004: Delele *et al*., 2005; Cerruto, 2007; Pergher and Petris, 2008; Dekeyser *et al*., 2012, 2013; García-Ramos *et al*., 2012, 2018; Gu *et al*., 2012; Pascuzzi, 2013; Duga *et al*., 2015; Garcerá *et al*., 2017; Hołownicki *et al*., 2017; Miranda *et al*., 2017, 2018; Balsari *et al*., 2019; Badules *et al*., 2018). But they do not serve to determine the direction of airflow or to detect turbulent structures. In this sense, the ultrasonic anemometers allow to calculate the value and the sense of each one of the components of the velocity. These sensors have been used successfully to describe the general airflow generated during the treatments, (Endalew *et al*., 2010b; Dekeyser *et al*., 2012, 2013; García-Ramos *et al*., 2012, 2018; Czaczyk *et al*., 2014; Salcedo *et al*., 2015; Triloff, 2015, 2016 and 2018; Garcerá *et al*., 2017; Van de Zande *et al*., 2017).

Seeking greater airflow to work at high forward speeds, axial fan sprayers for fruit trees are also used in vineyards (Grella *et al*., 2017). In this way, Landers and Farooq (2004) and Balsari *et al*., (2008) studied the relationship between the airflow characteristics and the canopy. On the other hand, Pergher, (2006), Cerruto (2007), and Pascuzzi (2013) analysed the effect of the movement and the airflow on the spray deposition in vineyards;

however, they focused on the air volume rates and not the sprayer airflow description. Therefore, it is necessary to understand the relationship of the generated air with the sprayer speed and the airflow penetration into the canopy. The initial step should provide a description of the airflow, as it leaves the sprayer from a plane directly aligned with the axial fan, to help visualize the physical phenomena in a better way.

The objective of this work was to establish an introductory study to understand the behaviour of airflow using an axial fan sprayer, built with an air assistance inverter system, in the air outlet plane of the fan and simulating an specific interval during plant protection treatment in vineyard trellis by means of ultrasonic anemometers. Hence, the air velocities, before and after crossing the canopy of artificial vineyards on both sides, were studied. The air velocities were characterized first with the sprayer stopped and then with the sprayer in a dynamic position. Results were compared to study the evolution of the airflow generated. The resistance showed by the vegetation was also characterized and compared between cases.

2. Material and methods

2.1. Experimental location

The tests were carried out at the Laboratory of Agricultural Mechanization belonging to the facilities of Agropolis of the Universitat Politècnica de Catalunya in Viladecans in Spain (41°17′18.44″N/2°2′43.39″W).

2.2. Artificial canopy

Two identical, artificial vineyard canopies of rectangular prism shape were used for the trials (Figure 1). Typical parameters in the region were considered for the canopy design. A theoretical vineyard case with a separation of 1.2 m between plants and 2.8 m between rows was selected. This section has already been used in previous air tests to reproduce treatments in vineyard trellis with good results (Gil *et al*., 2015). The leaf area index (LAI) was set at 1.0, which is within the typical range for vineyards (López–Lozano *et al*., 2009). This means that a 3.36 m^2 ground surface area is covered by a total leaf area of 3.36 m^2.

To achieve this, the canopies designed were 1.2 m long, 1.0 m high, and 0.4 m wide. A metal support 0.5 m serves as the platform for each canopy, giving the canopies a total height of 1.5 m from the ground surface. Each canopy had 540 leaves with an individual area of 67.6 cm^2. The leaf area density was α = 9.9 m^2 leaf m^{-3} canopy.

[Insert Figure 1]

2.3. Characteristics of the sprayer

A trailed airblast sprayer FEDE Inverter Qi 9.0 Ecoteqi (Fede S.L. sprayers, Cheste, Spain) connected to a Landini Rex 90F tractor (Landini SpA, Fabbrico, Italy) was used. The sprayer had a tank with a nominal volume of 2000 L (Figure 2).

[Insert Figure 2]

The machine has an air reverse system, with the suction fan was in front of the air outlet. Thus, the vectors of the airflow are more directed to the driving direction than the back compared to a treatment with a conventional airblast sprayer. It has an axial fan with a diameter of 900 mm and ten metal blades, each having an inclination angle of 20° that are rotated counter clockwise considering the rear position of the sprayer. The widths of its outlet and inlet channels are 185 mm and 300 mm, respectively, and the perimeter in both cases is 1.3m. The separation between channels is 0.2 m. The idea, with this design, is to avoid damages and obstructions in the sprayer by accumulation of leaves during the treatments in deciduous trees.

The sprayer was always working at a PTO (Power Take-Off) speed of 480 r min^{-1}, which is the value recommended by the manufacturer. The gearbox factor of PTO to fan is 1:4. The fan had two speed positions, but only the low speed was employed. In these conditions, the air volume rate was previously estimated, following the ISO 9898 methodology (ISO, 2000), by using a propeller anemometer Meteo Digit I (Lambrecht meteo GmbH, Göttingen, Germany). The total airflow rate obtained was of 10.7 m^3 s^{-1}, of which 53% corresponded to the right side of the fan at a mean velocity of 23.2 m s^{-1}, while 47% to the left side at a mean velocity of 20.6 m s^{-1}.

2.4. Measurements of air velocities

Static assays

For the static airflow test, both sides of the sprayer were considered. The machine was located equidistant to the two canopies (Figure 3). Thereby, the distance between the fan and the extreme of each canopy was 0.7 m. The air outlet was aligned with the centre of the canopies (plane z = 0.6 m).

[Inseret Figure 3]

The measurement procedure for the air velocities was based on the methodology proposed by Da Silva *et al*. (2006) for artificial vineyards. In the same plane of the air outlet (z = 0.6 m), the air velocities were measured at four posts (A, B, C and D) (Figure 3i). Two posts were stationed on each side of the sprayer: one between the fan and the canopy (B and C) and the other after the vegetation (A and D). Da Silva *et al*. (2006) placed these posts 0.1 m from the vegetation, but owing to difficulties inherent to the installation of the measurement sensor, they were positioned 0.2 m away on each side. The posts directly facing the fan (B and C) were located 0.5 m away from the sprayer, as proposed by ISO 9898 (ISO, 2000) for the characterization of the air blast sprayer (Figure 3ii). In each post, the air velocities were measured every 0.3 m, from 0.5 m to a maximum height of 2.0 m. Moreover, there were 6 measurement points for a total of 24 points in the plane z = 0.6 m.

At each of these points, a three-dimensional (3D) ultrasonic anemometer (WindMaster 1590-PK-020, Gill Instruments Ltd., Hampshire, UK) attached to the post was placed in a horizontal position. The sensor accuracy was 1.5%, with an air velocity range of 0 to 45 m s^{-1}, a resolution of 0.01 m s^{-1} and a frequency of 10 Hz. The three instantaneous components of air velocity (u_x, u_y, u_z) (m s^{-1}) were recorded, with the positive X-axis as the horizontal direction to the vegetation and parallel to the ground, Y-axis as the vertical component to the atmosphere, and Z-axis the horizontal direction following the sprayer and the tractor.

The static test included three repetitions to ensure that the general behaviour of the air was being characterized. The trials were executed by first measuring all points of A with the fan running. Then, the same process was executed for posts B, C and D. After D, the cycle was repeated two more times. This was done necessary to try to make the measurements at each point as independent as possible between repetitions. For each repetition, the acquisition time was 60 s at each measurement point, with a sampling frequency of 10 Hz (600 data).

Dynamic assays

For the dynamic tests, the positions of the canopies and the posts were kept in the same positions (Figure 4). The sprayer passed between the two vineyards rows maintaining the same distance to the vegetation as in the static assay. For the forward speed, a value of 1.14 m s^{-1} (4.1 km h^{-1}) was chosen. This value has been used in previous assays to study the airflow during a typical treatment in the region (Gil *et al*., 2015), which is within the range of speeds for the local farmers.

[Insert Figure 4]

Previous studies were considered for establishing the number of repetitions required for the tests. For instance, Endalew *et al*. (2010) performed a total of 18 repetitions for a air-assisted sprayer circulating at more than 1.94 m s^{-1} (7.0 km h^{-1}). On the other hand, García-Ramos *et al*. (2012) carried out much less, 3 repetitions, although the sprayer was 0.77 m s^{-1} (2.8 km h^{-1}). For this first approach, it was considered that our conditions were more similar to the work of García-Ramos *et al*. (2012) who used the same 3D-ultrasonic anemometer model as this trial but with a frequency of 1 Hz. Thus, based on that study, five repetitions were performed for each point. In each repetition, only the velocities that the anemometer captured were recorded because the air outlet channel coincided with the vegetation until the air left the vineyards. Given the forward speed and the length of the vineyard (1.2 m), the estimated time of measurement was approximately t = 1.1 s.

2.5. Environmental conditions during the experiments

The trials were conducted in accordance to the best management practices recommended for a good and safe spray application process (TOPPS–Prowadis, 2014). This implies that wind speed be lower than 3 m s^{-1} during the application (BOE, 2012). With respect to the orientation of the spray track to the wind direction during the tests, the wind velocity and direction were measured at 0.1 Hz frequency sampling rate. To record the variables during the experiment, an automatic weather station (WatchDog weather station Model 2550, Spectrum Technologies, Inc., USA) was used. The station was placed at 25 m downwind from the equipment at a height of 2.0 m. The mean wind velocity during the static trials was 1.8 m s^{-1}, and the mean direction was 201° relative to the travel direction of the sprayer. During the dynamic assays, the values were 1.4 m s^{-1} and 175º, respectively. The environmental wind affects measurements that depend on height (Georgiadis, Dalpane, Rossi, Nerozzi, 1996). Nevertheless, Endalew *et al*. (2009) suggested that this effect is only significant above 1.5 times the height of the canopy (in this case, at 2.25 m), which has been successfully applied in other air assays (Salcedo *et al*., 2015). Therefore, this effect was treated as negligible considering the mean wind velocity obtained during the tests and the maximum height for the measurements (2.0 m).

2.6. Data processing

<u>*Static data*</u>

For each repetition, the airflows during the static test were assured to be within the steady state so that the air velocities represented the behaviour of the airflow correctly. For each measurement point (Fig. 3), the cumulative average of each velocity component was calculated up to 60 s. Afterwards, the mean behaviour during that time was studied, to observe whether it moved within the same range, in the same order of magnitude, as the mean value, after 30 s. If the data continued to increase or decrease until 60 s, then it meant that the steady state had not been reached at that point, and thus, the data would not be considered.

To graphically represent the airflow during the tests, the total mean velocities for each component (U_{Tx}, U_{Ty}, U_{Tz}) (m s^{-1}) between the repetitions were calculated. From these velocities, the total mean velocity magnitude in each point was obtained:

$$U_T = \sqrt{U_{Tx}^2 + U_{Ty}^2 + U_{Tz}^2} \quad (1)$$

Two diagrams (with the corresponding air velocity vectors) that coincide with each of the measurement planes were generated. One was for the plane $z = 0.6$ m, using the coordinates of the mean velocities U_{Tx} and U_{Ty}. This diagram reflected the behaviour of the airflow to the target vegetation. The other graph was for each post in the planes $x = -1.75$ m, $x = -0.95$ m, $x = 0.95$ m, and $x = 1.75$ m. These diagrams used the mean velocities U_{Ty} and U_{Tz} and showed the airflow in the plane parallel to the machine.

For each repetition, the fluctuation of the air velocity u' (m s^{-1}) at a point can be expressed as the relation between the mean value U (m s^{-1}) and the instantaneous velocity u (m s^{-1}) measured by an anemometer, as in the following equation:

$$u' = u - U \quad (2)$$

The parameter u' is defined as the magnitude of the fluctuations in the three components:

$$u' = \sqrt{\frac{1}{3}\left(\overline{u'_x u'_x} + \overline{u'_y u'_y} + \overline{u'_z u'_z}\right)}, \quad (3)$$

where $\overline{u'_x u'_x}$, $\overline{u'_y u'_y}$ and $\overline{u'_z u'_z}$ are respectively the square of the fluctuation in each direction of the space. For the fluctuations, the airflow was assumed to be isotropic, which means that the variations in the components are similar to each other.

Based on Eq. (2), it is possible to obtain the turbulence intensity I (%). It is expressed as

$$I = 100\sqrt{\frac{1}{3}\left(\overline{u_x^{'}u_x^{'}} + \overline{u_y^{'}u_y^{'}} + \overline{u_z^{'}u_z^{'}}\right)} / \sqrt{\left(U_x^2 + U_y^2 + U_z^2\right)} \qquad (4)$$

where (U_x, U_y, U_z) (m s^{-1}) are the mean values for each repetition. This variable is a ratio used to compare the importance of the fluctuations on the mean velocity of the airflow. Finally, the total mean intensity I_T between the repetitions was represented.

Dynamic data

To simulate a representative moment during a treatment in vineyard trellis, only air velocities were considered when the fan was between the two canopies. Considering the sensitivity of air measurements in the dynamic test and the possible errors that may occur during the measurements (error in the equidistance to the vegetation, the difficulty of keeping the forward speed constant, precision in data collection at the time of defining the fan inlet facing the vineyard canopies), it was decided that an estimate of the average behaviour of the airflow when the fan inlet moved in three different sections (Figure 5): previous zone (from z = 0.0 to z = 0.4 m) called Z1, central or Z2 (from z = 0.4 m to z = 0.8 m) and posterior or Z3 (from z = 0.8 to z = 1.2 m), be made.

[Insert Figure 5]

The estimated total mean velocities were characterized analogously as in the static test. The turbulent intensities were estimated following Eq. (3).

The resistance that the vegetation presents to the sprayer airflow can be characterized by a drag coefficient C_d (-). To obtain this value, the methodology proposed by Da

Silva *et al.* (2006) was used, who applied it in an experiment with an axial fan sprayer and artificial vineyards:

$$C_d = \frac{1}{\alpha L} ln\left(\frac{U_{Txa}}{U_{Txb}}\right), \quad (4)$$

where L (m) is the depth of the canopy, α is the leaf area density (m^2 leaf m^{-3} canopy), U_{Txb} the mean horizontal air velocity prior to canopy penetration (in this case, B and C) and U_{Txa} after the vegetation (A and D).

The final results obtained between the static and dynamic tests were compared. The data compared were the air velocities for the static experiment and those for the central zone in the dynamic test. Variation between velocity magnitudes, angles between the vectors, and drag coefficients and differences between intensities and drag coefficients were calculated.

3. Results and Discussion

3.1 Static assays

<u>*Total mean velocities*</u>

For all posts, U_T decreased with height (Figure 6). The horizontal component had the largest value. The influence of U_{Tx} was predominant in the area closest to the ground; however, the importance to the component U_{Ty} reduced as the height increased.

[Insert Figure 6]

The air velocities registered before crossing the canopies (posts B and C) decreased between the lowest (0.5 m) and the highest (2.0 m) points. The maximum velocity between these posts was observed on the right side (post C) at 0.5 m. The same trend was observed on at 0.8 m on the left side (post B). In addition, post B, the velocities increased again at 1.7 m. In general, the velocities were always higher the left side owing to the counter-clockwise direction of the fan, which provided more energy to the airflow on this side.

After the airflow passed through the canopies, the velocity values were very close to each other on both sides of the sprayer at all heights. The losses produced by the vegetation decreased the energy of the air. Furthermore, the airflow was found to exhibit a more symmetrical behaviour than those at post B and C. This is also observed in the values of U_T at each post in Table 1. This similarity, which is also observed above the canopies, could be interesting from the point of view of the lower boundary layer of air. This could indicate that the influence of the airflow of the fan on the droplets over the canopies was very similar on both sides, despite the differences before going through the canopies. In addition, this behaviour after the canopy contrasted with the differences obtained in posts B and C, especially in higher points. It could suggest that, for this range of velocities, the effect of the vineyard on the air was not noticeable at the canopy entrance, unlike other crops with higher density such as citrus (Salcedo *et al*., 2015). In this way, it is necessary to deep in the interaction between air velocity and vegetation to determine which is the minimum value to cross the vegetation to ensure a good penetration of the airflow into the vineyards without negative effects on the droplets penetration or the drift above the canopy as indicated Balsari *et al*., (2008) and Triloff (2015).

Another point of discussion is that the velocities were larger in B than in C, while measurements with the propeller anemometer in the fan outlet, to calculate the air volume rate, recorded the biggest values in the right side of the sprayer. However, only one plane velocities are being measured (z = 0.6 m). Several works have shown the high variability of airflow behaviour when studying air in different parallel planes (Salcedo *et al*., 2015; Triloff, 2016; Van de Zande *et al*., 2017). Probably, if the air velocities in other parallel planes were included, it would be observed how the right side was bigger. For future works more parallel planes should be included. In addition, the fan asymmetry should also be considered. It could be that the anemometer was not facing the main airflow in the same way on each side. This asymmetry could also be affected with the presence of the suction zone in front of the air outlet. Personal experiences with conventional sprayers showed that static airflow has a positive U_{Tz} component. The air reverse system could be intensifying this component, diverting more airflow to the tractor and increasing the differences in measurement on both sides. Thus, the inclination of the plane of the airflow outgoing of the fan to the central axis of the machine (x = 0) in a static test should be defined in news field assays.

Table 1. Values of the velocity magnitudes in each post during the static assay.

Magnitude velocity	**Values (m s^{-1})**			
	Post A	**Post B**	**Post C**	**Post D**
Total mean	4.7	13.1	9.0	4.9
Standard deviation	1.5	2.8	2.7	1.7
Maximum	10.1	21.8	18.8	11.9
Minimum	1.7	5.4	2.6	1.5
Mode	4.3	12.3	9.3	4.9

Plane XY

The airflow direction on both sides of the machine (Figure 7) was always similar: The airflow advanced in the direction of the vegetation, oriented towards the ground, then went up the first third of the height of the canopy where the air ascended. The data were displayed in Fig, 6 and Table 1. The airflow on the left side of the fan was more intense than those on the right side; however, after crossing the canopies, they had a more similar profile. The predominant influence of U_{Tx} was also displayed.

[Insert Figure 7]

The vegetation resistance was not large enough to produce an airflow separation, in which case vortexes around the canopies are formed, as in the case for other crops such as orange trees (Salcedo *et al*., 2015), in which vegetation is denser and the canopies have a larger diameter. No screen effect on the air was observed, unlike in denser crops such as orange trees, where the airflow moves towards the atmosphere owing to difficulty in crossing the vegetation.

On the other hand, the airflow behaviour in front of and behind the canopies did not completely coincide with the results obtained by Da Silva *et al*. (2006) in a similar vineyard setting. Although in that experiment U_{Tx} was also positive, the velocities formed a depression in the section coincident with the height of the canopy. These differences were confirmed by Da Silva *et al*. (2006). The authors in the aforementioned study worked with a lower average velocity range (7.0 m s^{-1}) than that in the present work (Table 1), with the airflow focused directly on the vegetation, and with a larger canopy diameter (L = 0.7 m).

Plane ZY

The U_T vectors always presented a positive U_{Tz} component in all the positions (Figure 8). In both sides, the airflow was not parallel to the plane coincident with the air fan outlet (z = 0.6 m). In addition, the airflow reflected that it was oriented to the direction of the sprayer before or after the vegetation.

[Insert Figure 8]

Considering posts B and C, the velocities on the right side were found to be more intense than on the left side. This reinforced the hypothesis that the air was more aligned with the anemometer on one side than on the other. In addition, the suction zone of the air reverse system was probably intensifying the velocities U_{Tz}. On the other hand, in A and D, the effect of the vegetation was not enough to cause changes in the airflow direction after the canopy.

<u>*Turbulence intensity*</u>

The I_T intensities displayed an opposite profile from the velocities (Figure 9). The sections where the velocities presented the highest values coincided with the area in which the turbulent intensity was the lowest. This could be explained because, given the constant airflow produced by the fan within the stationary regime, the higher the velocity at a point, the lower the effect of the fluctuations on the average velocity. The most unstable areas, which had a higher value of I_T, were located above the canopy, which was the area of with the greatest risk, considering the spray drift.

[Insert Figure 9]

In Fig. 9, the intensities before the vegetation were similar at 0.5 m. However, the intensities increased differently between posts B and C. This indicates that the turbulence of the air was not similar on both sides of the fan. The intensity in the post C continued to increase above the vegetation, while it fell again in the post B. The airflow on the right side became more unstable as the height and distance from the machine increased.

After the vegetation, the I_T intensities exhibited a similar profile on both sides of the machine with the behaviour of UT as shown in Fig. 5. The most stable zone on both sides was between the heights of 0.5 m and 1.1 m. However, when reaching the upper part of the canopy from 1.4 m, I_T increased at a faster rate coinciding with the absence of obstacles in front of the airflow. The vegetation could be producing losses in air velocity, which meant that the fluctuations were also smaller, which resulted in a decrease of their influence over the average air velocity.

Drag coefficient

The calculated drag coefficient C_d in the canopies for the artificial vegetation was 0.24 on the left side and 0.16 on the right side. This difference in value between canopies coincided with the largest velocities recorded on the left side. The higher the velocity gradient between the inlet and the outlet of the canopy, the higher the drag coefficient, indicating that the vegetation produced more losses on the left side than on the right side. Da Silva *et al*. (2006) indicated that the typical values range between 0.1 and 0.5. In their experiment, C_d = 0.3. Considering this information, it was concluded that the values obtained during the field tests corresponded to those expected in this case. Thus, it was considered that the artificial canopies had resistance similar to real vegetation.

3.2 Dynamic assays

Total mean velocities

When the fan outlet was in zone Z1, the U_T velocities at z = 0.6 m were lower than those obtained for the static test (Figure 10i). However, the maximum values measured in A at 2.0 m and in B at 1.4 m were probably produced by the influence of the sprayer airflow.

Both posts were on the left side, which was the side having the most intense velocities in the static test (Figure 7). On the contrary, the velocities behind the canopy in C, which were more exposed to the suction phenomena of the fan, were higher than in D (Table 2). The horizontal component U_{Tx} was predominant in these values.

[Insert Figure 10]

In the central part (zone Z2), U_{Tx} followed the main component in U_T. The velocities detected in B were up to four times higher than those measured from 0.8 m in the other posts (Figure 10ii). The maximum value occurred at a height of 1.1 m, as obtained in the static test, and then started descending. However, the maximum velocity recorded was 50% lower than U_T measured in the static test.

On the contrary, all velocities in C were lower than 2.0 m s^{-1}, as indicated in Table 2, except at 1.1 m, where the biggest value was registered, as that in B. These data seemed to reflect the asymmetry that can be detected at the fan outlet during the pesticide treatment. This could mean that the droplets coming out of the nozzles on either side of the machine do not receive the same amount of energy from the air flow. This aside, behind the canopy, U_T continued to descend below 2.0 m s^{-1} as in Z1.

In the last part (zone Z3), the behaviour of U_T in B was reversed (Figure 10iii). There was minimum U_T at 1.1 m, and then it went up to 6.0–8.0 m s^{-1} between 1.7 m and 2.0. The outgoing flow at the same height coincident with the fan was more intense than in Z2. The data in Z3 suggested that the movement of the sprayer was displacing the airflow toward the direction opposite to the advance. For this reason, the sprayer airflow influence was detected in the next zone Z3. In contrast, the velocities in A increased similarly to those of B in Z2 due to the increase in the vertical component U_{Ty}. On the right-side canopy, the maximum value of U_T above 10.0 m s^{-1} was detected in C at 1.1 m, while for the rest of the points, the velocities did not decrease from 4.0 m s^{-1}. In D behind the canopy, the values were bigger than those observed in Z2, although there was a minimum at a height of 1.1 m, contrary to the case of C. Therefore, the airflow on the right side did not seem to follow a uniform structure.

Table 2. Total mean velocity magnitudes in each post during the dynamic assay

Magnitude velocity	**Values (m s^{-1})**											
	Post A			**Post B**			**Post C**			**Post D**		
	Z1	**Z2**	**Z3**	**Z1**	**Z2**	**Z3**	**Z1**	**Z2**	**Z3**	**Z1**	**Z2**	**Z3**
Total mean	0.9	1.2	3.1	1.5	4.6	5.2	1.3	1.6	7.7	0.7	0.8	3.4
Standard deviation	0.7	1.1	2.2	0.9	4.8	4.2	0.3	2.1	5.7	0.3	0.9	2.7
Maximum	3.6	6.4	11.0	7.4	20.5	19.1	2.0	13.7	22.6	1.6	6.3	10.3
Minimum	0.1	0.1	0.6	0.5	0.6	1.0	0.8	0.6	0.2	0.3	0.2	0.1
Mode	0.4	1.7	1.8	1.2	2.2	3.3	1.4	1.1	13.4	0.9	0.7	5.0

To explain why the velocities measured in Z3 were bigger than in Z1 and Z2, it can consider different factors such as the air reverse system, with the suction zone closer to the tractor than the fan outlet, the forward speed of the sprayer, influencing on the velocities variation as it was indicated in other works (Delele *et al*., 2005; Triloff, 2011; Gu *et al*., 2012) or the resistance of the vegetation, as it was considered in CFD simulations (Endalew *et al*., 2010; Hong *et al*., 2018). In this way, it is necessary to carry out more test to estimate the influence level of these factors.

<u>*Sprayer airflow characterization*</u>

<u>Plane XY</u>

When the fan was located at Z1, the XY velocity vectors demonstrated different behaviours on both sides of the sprayer (Figure 11i). On the right side, the vectors of UTx and U_{Ty} always moved toward the fan. As the suction zone was ahead of the fan outlet, this could be conditioning the airflow in D and, more intensively, in C. On this side, the presence of the canopy itself was not enough to produce an airflow separation and form turbulent structures around it.

On the contrary, on the left side in both posts, the airflow reflected the same characteristics: the vectors were oriented opposite to the fan at the highest points and were changing their directions towards the machine as the height was reduced. This behaviour is typical when a vortex appears (counter-clockwise in this case). There were two vortices—one before and one after the vegetation—probably due to the separation of airflow generated by the presence of the canopy since the airflow was not strong enough to overcome the resistance.

The presence of these turbulent structures on one side but not on the other side was caused by the asymmetrical air output of the moving equipment. On the other hand, the negative values of U_{Tx} in B and, mainly, in C could be affected by the suction zone in front of the fan air outlet.

[Insert Figure 11]

In Z2 (Figure 11ii), the U_{Tx} on the left side progressed towards the vegetation. The resistance of the vegetation was not sufficient as to produce turbulent structures around it. However, it was observed that the vectors in A had less presence in the height coincident with the canopy. The vegetation produced velocity and pressure losses on the airflow. Meanwhile, turbulent structures before and after the canopy were recorded on C and D, with U_{Tx} changing with respect to the height. At this instance, the outgoing flow on the right side was not measured in the plane $z = 0.6$ m yet. This turbulent behaviour resembled with that observed on the left side in Z1, with turbulent formations around the canopy before receiving the main air jet. In addition, this asymmetric behaviour suggested that the droplets coming out of the nozzles received a different influence from the air on both sides.

With the air outlet in Z3 (Figure 11iii), the velocity vectors on both sides left the sprayer towards the vegetation. The U_{Ty} was positive at the upper part of B and negative at 0.5 m. These results, next to the velocity magnitudes shown in Figs. 10ii and 10iii, seemed to reinforce the three-dimensional (3D) behaviour of the sprayer airflow, as indicated by Delele *et al*. (2005), due to several parameters such as the presence of obstacles or the forward speed. The vectors obtained suggested that the airflow would leave the fan and form a 3D structure like a regular hollow half-cone, which would expand as the machine advanced, while the airflow from the medium height of the fan would move away from the machine. In this case, the outgoing airflow expanded at 0.5 m and 2.0 m and moved away from the fan, as shown from the vectors with higher magnitudes in A. This hypothesis was reinforced with the CFD simulations on applying treatments to trees with sprayers, performed by Endalew *et al*., (2010b). The simulations reflected an isosurface to present the air jet with a shape that matched with the results obtained for the dynamic experiments conducted in this study.

However, it should be taken into account that all these turbulent structures are produced considering a hypothetical continuous row such as in vineyard trellis. It would be interesting to compare these results not only with real vegetation but also with other types of crops, such as vineyards in hedge, especially for Z1 and Z3.

Plane ZY

The velocity vectors ZY in Z1 showed that U_{Tz} was lower than U_{Tx} and U_{Ty} (Figure 12i). This indicates that the flow from the fan in this position flowed very perpendicular to the machine. As in the static assay (Figure 8), U_{Tz} was positive in A, B and D, while it was negative in C. The movement of the sprayer reinforced the asymmetric behaviour of the fan with respect to the static test. Probably this was due to air suction phenomena, produced by the air reverse system of the fan, and the scarce presence of the air outgoing of the fan in that post. If in the static assay the air left the fan in the direction of the sprayer, in the dynamic experiment the airflow moved in the opposite direction in C. The difference between C and D indicated that the influence of the fan was still low, as suggested by the data in the Figure 11i. In addition, the vectors were more intense on the left side, where vortices in XY were present, than on the right side of the sprayer.

[Insert Figure 12]

In the central zone Z2, a similar behaviour for U_{Tz} was observed, except in B, where the magnitude of the velocities increased and where all the vectors had the same direction coincident with the larger flowing air volume in XY (Figure 11ii). The vectors in A, B and D moved in the same direction as in the static test (Figure 8). However, the vectors in all the posts were smaller than those in the static test, probably explained by the deviation of the airflow to the back part and the dissipative effect produced by the movement and the interaction with the air currents around the sprayer, as in the XY plane (Figure 11ii).

Finally, the U_{Tz} vectors in B in Z3 were observed to change the direction from the bottom to top (Figure 12iii), which indicates that the airflow became closer to the machine as the height of the post increased, while in C, vectors were always in the direction opposite to the advance of the sprayer. The field data after the canopies suggested that the airflow dissipated earlier on the right side than on the left, as reflected by the variation in the direction of the vectors in D with respect A.

Turbulence intensity

In Z1, the lowest turbulence intensities occurred in the posts on the right side (Fig. 13i), where the U_T vectors exhibited a more stable behaviour (Fig.11i and 12i). This shows that the airflow was in the horizontal direction towards the sprayer. In contrast, I_T reached the highest values on the left side, where there were vortices before and after the vegetation. It means that the magnitude of the fluctuations exceeded the average velocity in these points.

When the sprayer was in the central part Z2, the I_T values became larger than those in Z1 (Figure 13ii). The highest values were measured in C and D, where vortices were present (Figure 11i). The increase in velocity on the left side coincided with the increment of the fluctuations in the airflow. The increase of the mean velocities was lower than the enhance of the fluctuations. Thus, posts C and D during Z2 presented the most turbulent behaviour during the trials.

[Insert Figure 13]

In Z3, the maximum values on the right side were registered at the upper and inner points of the posts (Fig. 13iii). The airflow seemed more stable along the height coincident with the fan, where the velocity was higher (Fig. 10iii). In A and B, I_T decreased with respect to Z2. Therefore, the airflow leaving the fan on the right side showed fewer fluctuations in this area.

Anyway, future works using anemometers with higher frequency, and more passes and measurement points, are necessary to study in greater depth the turbulent behaviour of the airflow, especially during the movement of the sprayer.

Drag coefficient

When the fan was located in Z2, C_d was similar on both canopies: 0.17 in the left and 0.19 in the right canopy. In the dynamic test, the velocity gradients were reduced although the behaviour of the velocity vectors on either side of the canopy differed (Figure 11ii). This could be because the U_T velocities were smaller considering the magnitude in the dynamic assay (Table 2) and the differences between velocities were smaller on each side of the vegetation. Even so, these values were still within the usual range in the literature (Da Silva *et al.*, 2006).

3.3. Comparison between static and dynamic assays

Magnitudes

Taking Z2 as a reference for the comparison of the dynamic and static tests data, the U_T velocities in the posts before crossing the vegetation showed a similar tendency in B on the left side of the sprayer (Figure 6 and 10ii) and reached a maximum at 0.8 m. However, in C of the dynamic assay, U_T reached 2.5 m s^{-1} (Table 2), while it reached more than 15.0 m s^{-1} in the static test (Table 1). There were more similarities in values in both posts in Z3.

After the canopies, the velocities above the vegetation in A were similar. However, the velocities in the dynamic experiment were up to three times lower than those in the static one. The same trend was observed in D. In the static test, the U_T components increased until they reached a maximum and then decreased. In the dynamic assay, they were lower although stable within the 0.4–2.0 m s^{-1} range. In addition, as in the static test, the velocities in A and D were closer to each other above the vegetation.

The results showed that the sprayer airflow, considering the velocity magnitude, resembled more the static test in Z3 than in Z2. In this case, U_{Tz}, although the lowest component, played an important role because its behaviour could determine how the airflow could be reflected in the central plane of the fan.

Table 3 shows how the magnitude of the ZY vectors deviated between 37% (A) and 76% (B) between the static and dynamic assay (Fig. 8 and 12ii). During the static test, the magnitudes were larger. But, during the dynamic assay magnitudes were lower, which implies that the outgoing sprayer airflow was more aligned with the plane z = 0.6 m during the static experiment.

These differences are concordant with those of De Moor *et al*., (2002), García-Ramos *et al*., (2012) and Gu *et al*., (2012) who described a decrease in the magnitudes of the static experiment in comparison with dynamic assay, being more noticeable with increasing forward speeds. Thus, as Table 3 indicates, the movement of the sprayer reduce the air velocity at the canopies, according with the observed in other studies (Delele *et al*., 2005; Triloff, 2011). This should also motivate to the manufacturers to evaluate if it is logical to design the airflow of the fan considering only the parameters of the crop and not the forward speed of the sprayer. Therefore, future works to carry out more dynamic trials are necessary to estimate the relation between the forward speed and the air velocities considering the characteristics of the crop and the sprayer.

Table 3. Average deviation rate of the magnitudes of the XY and ZY vectors of the dynamic test (Z2) with respect to the static assay.

Plane	Average deviation (%)			
	Post A	Post B	Post C	Post D
XY	77.6	65.3	76.1	87.0
YZ	9.2	68.3	75.2	76.3

Angles between vectors

The biggest differences between vectors U_T in the XY plane were produced on the right side (Table 4), as shown in Figs. 7 and 11ii. The airflow on the left side of the fan (posts A and B) moved away from the equipment while the velocity vectors moved towards the vegetation and inclined towards the atmosphere as the height of each post increased. Even the differences were smaller if the values at 1.1 m and 0.5 m in posts A and B, respectively, were not considered. With respect to the most stable flow in the static test, the vortices detected in C and D explained the differences greater than 100º.

Likewise, in the ZY plane, the highest angles between vectors were also in C and D, while the smallest differences occurred against the left side of the fan. On the other hand, differences with respect to the static assay were lower in B and C than in the plane XY. It could be because the air reverse system was reducing the effect of the movement of the sprayer on the direction of the airflow, more oriented to the driving direction than the back compared with a conventional axial fan sprayer.

Table 4. Average angles between the XY and ZY vectors of the dynamic test (Z2) with respect to the static assay.

Plane	Average angle (º)			
	Post A	Post B	Post C	Post D
XY	40.7	37.6	103.0	119.1
YZ	51.5	35.5	81.9	136.5

Turbulence intensity

Comparing Figs. 9 and 13ii, in the static test the intensities decreased as the velocities increased in magnitude, whereas in the dynamic test this did not happen, especially in Z2. Therefore, it seemed that the movement of the equipment resulted in more instability to the airflow. The data indicated that the fluctuations in the dynamic assay increased proportionally to the average velocity. Nevertheless, the influence of the vegetation length in this work must be taken into account. Future work is needed to observe the turbulent behaviour of airflow in longer vineyard rows.

Drag coefficient

The drag coefficient in the left canopy was reduced by 30% when shifting from static to dynamic, while in the right it increased by approximately 20%. The decrease in the air velocity magnitude during the dynamic assay and the behaviour of U_{Tx} did not seem to affect the coefficients on both sides of the fan when the sprayer was moving. On the other hand, the drag coefficients in the dynamic experiment were more similar to each other. The resistance offered by the canopies on both sides could then be considered equal. In these assays seemed that the drag coefficient influence on the airflow was approached on both sides of the sprayer, especially with the ability of vegetation to divert the airflow into the surrounding air. On the other hand, it is necessary to new assays comparing the drag coefficient with rows longer than 1.2 m to eliminate possible edge effects of this artificial canopy.

4. Conclusions

A static and dynamic study of the airflow produced by a sprayer with an axial fan and an air reverse system was carried out using artificial canopies of vineyards. Ultrasonic anemometers were successful in characterizing sprayer fan airflows.

The results showed that when the sprayer was working in a static position, airflow on both sides of the equipment came from the machine and crossed the vegetation, with the turbulence intensity decreasing as the air velocities increased. In addition, the air velocity vectors, were slowed down by the vegetation. But before crossing the canopies, the vectors *XY* (plane perpendicular to the sprayer) were more intensive on the left side and vectors *ZY* (parallel to the sprayer) on the right side. Airflow presented positive components in *X*-axis (to the vegetation) and *Z*-axis (to the sprayer). In the case of the component *Z*, the suction zone of the air reverse system could be affecting.

With the sprayer in motion, the air velocity magnitude was reduced, and turbulent structures were generated around the vegetation. The biggest velocity vectors in *XY* coincided with the vectors in opposite direction to the sprayer in *ZY*. The asymmetry increased and the outgoing airflow on the right side was not in the same plane as the one on the left side. The outgoing airflow manifested more in the direction opposite to that of the advance of the sprayer.

In the field experiments it was found that, after crossing the vegetation when the canopy received the direct airflow, the air velocity vectors moved in a similar magnitude and direction. This suggested that the risk of lower boundary layer of air and the influence on the displacement of the pesticide droplets could be similar to both sides of the sprayer, despite the asymmetry of the air leaving the fan.

Regarding the turbulence intensity of the air, in the static test, the areas with the highest air velocity had a lower turbulence intensity but it was not fulfilled in the dynamic test. The movement of the sprayer had a direct effect on the turbulence intensity and the variability increased with the velocity of the airflow.

During the static and dynamic tests, the drag coefficients presented similar values in both canopies. This could mean that their ability to influence the trajectory of airflow, especially those that could not pass through the vegetation and be diverted to the surrounding air, was similar on each side of the fan.

It is necessary to continue working on the descriptive analysis of the airflow by:

- defining the inclination of the plane of the airflow outgoing of the fan to the central axis of the machine ($x = 0$) in a static test;
- increasing the frequency of anemometers, to deepen the dynamic behaviour of the airflow, and the number of passes during the dynamic experiment to confirm the hypotheses obtained here. Additionally, other aspects such as the variation of the distance of the fan to the canopies, the length of the vegetation, fan speed, PTO, airflow rate or the forward speed of the sprayer should be further examined. The resolution of the measurement grid, including more planes in Z-axis, acquisition time, and the number of passes required should also be defined;
- studying the interaction between air velocity and vegetation to determine which is the minimum value to cross the vegetation to ensure a good penetration of the airflow into the vineyards without negative effects on the efficiency of the treatment;

- comparing the results with other prototypes of air-assisted sprayers and different crops such as vineyards in hedge.

Acknowledgments

This research was developed under the collaboration Pulverizadores Fede SL.

References

Badules, J., Vidal, M., Boné, A., Llop, J., Salcedo, R., Gil, E., García-Ramos, F.J., 2018. Comparative study of CFD models of the air flow produced by an air-assisted sprayer adapted to the crop geometry. Comput. Electron. Agric. 149, 166-174.

Balsari, P., Marucco, P., Oggero, G., Tamagnone, M., 2008. Study of optimal air velocities for pesticides application in vineyard. Asp. Appl. Biol. 84, 417-423

Balsari, P., Grella, M., Marucco, P., Matta, F., Miranda-Fuentes, A. 2019. Assessing the influence of air speed and liquid flow rate on the droplet size and homogeneity in pneumatic spraying. Pest Manag. Sci. 75, 366-379.

Belcher, S.E., Jerram, N., Hunt, J.C.R., 2003. Adjustment of a turbulent boundary layer to a canopy of roughness elements. J. Fluid Mech. 488, 369-398.

BOE (Boletín Oficial del Estado), 2012. Real Decreto 1311/2012, de 14 de septiembre, por el que se establece el marco de actuación para conseguir un uso sostenible de los productos fitosanitarios. BOE N 223 de 15 de septiembre de 2012, 65127-65171.

Brazee, R.D., Fox, R.D., Reichard, D. L., Hall, F.R., 1981. Turbulent jet theory applied to air sprayers. Trans. ASAE. 24, 266–0272.

Carvalho, F.P., 2017. Pesticides, environment, and food safety. Food Energy Secur. 6, 48–60.

Celen, I.H., 2008. Effect of angle of sprayer deflector on spray distribution in dwarf apple trees. J. Agron. 7, 206–208.

Celen, I.H., Durgut, M.R., Avci G.G., Kilic, E., 2009. Effect of air assistance on deposition distribution on spraying by tunnel-type electrostatic sprayer. Afr. J. Agric. Res.

4, 1392–1397.

Cerruto, E., 2007. Influence of airflow rate and forward speed on the spray deposit in vineyards. J. Agric. Eng. 38, 7–14.

Chen, Y., Ozkan, E., Zhu, H., Derksen, R., Krause, C.R., 2013. Spray deposition inside tree canopies from a newly developed variable-rate air-assisted sprayer. Trans. ASABE. 56, 1263–1272.

Cross, J.V., Walklate, P.J., Murray, R.A., Richardson, G.M., 2001. Spray deposits and losses in different sized apple trees from an axial fan orchard sprayer: 1. Effects of spray liquid flow rate. Crop Prot. 20, 13–30.

Cross, J.V., Walklate, P.J., Murray, R. A., Richardson, G.M., 2003. Spray deposits and losses in different sized apple trees from an axial fan orchard sprayer: 3. Effects of air volumetric flow rate. Crop Prot. 22, 381–394.

Czaczyk, Z., 2012. Influence of air flow dynamics on droplet size in conditions of air assisted sprayers. Atomization Spray. 22, 275–282.

Czaczyk, Z., Bäcker, G., Keicher, R., Müller, R., 2015. Air flow characteristics–proposed as mandatory requirement for airblast sprayers. Julius-Kühn-Archiv. 168-171.

Da Silva, A., Sinfort, C., Tinet, C., Pierrat, D., Huberson, S., 2006. A Lagrangian model for spray behaviour within vine canopies. J. Aerosol Sci. 37, 658–674.

Damalas, C.A., 2015. Pesticide Drift: Seeking Reliable Environmental Indicators of Exposure Assessment. In: Armon, R., Hänninen, O., (Eds.), Environmental Indicators. Springer, Dordrecht, pp. 251-261.

Das, N., Maske, N., Khawas, V., Chaudhary, S.K., Dhete, E.R., 2015. Agricultural Fertilizers and Pesticides Sprayers-A Review. Int. J. Innov. Res. Sci. Eng. Techno. 1, 44-47.

De Moor, A., Langenakens, J., Jaeken, P., 2002. Dynamic air velocity measurements of air-assisted sprayers in relation to static measurements. Asp. Appl. Biol. 66, 309–322.

Delele, M.A., De Moor, A., Sonck, B., Ramon, H., Nicolaï, B.M., Verboven, P., 2005. Modelling and validation of the air flow generated by a cross flow air sprayer as affected by travel speed and fan speed. Biosyst. Eng. 92, 165–174.

Delele, M.A., Jaeken, P., Debaer, C., Baetens, K., Endalew, A.M., Ramon, H., 2007. CFD prototyping of an air-assisted orchard sprayer aimed at drift reduction. Comput. Electron. Agric. 55,16–27.

Dekeyser, D., Goossens, T., Melese Endalew, A., Verboven, P., Hendrickx, N., Nuyttens, D., 2011. Performance assessment of orchard sprayers, Part 1: Machine Characterization. 11th Workshop on Spray Application Techniques in Fruit Growing (Suprofruit), Bergerac, 8-10 June.

Dekeyser, D., Foque, D., Endalew, A. M., Verboven, P., Goossens, T., Hendrickx, N., Nuyttens, D., 2012. Assessment of orchard sprayers using laboratory trials. Asp. Appl. Biol. 114, 395-403.

Dekeyser, D., Duga, A. T., Verboven, P., Endalew, A. M., Hendrickx, N., Nuyttens, D. 2013. Assessment of orchard sprayers using laboratory experiments and computational fluid dynamics modelling. Biosyst. Eng. 114, 157-169.

Duga, A.T., Ruysen, K., Dekeyser, D., Nuyttens, D., Bylemans, D., Nicolaï, B.M., Verboven, P., 2015. Spray deposition profiles in pome fruit trees: Effects of sprayer design, training system and tree canopy characteristics. Crop Prot. 67, 200-213.

Butler-Ellis, M. C. B., Van de Zande, J. C., Van de Berg, F., Kennedy, M. C., O'sullivan, C. M., Jacobs, C. M., Fragkoulis, G., Spanoghe, P., Gerritsen, R., Frewer, L.j., Charistou, A., 2017. The BROWSE model for predicting exposures of residents and bystanders to agricultural use of plant protection products: an overview. Biosyst. Eng. 154, 92-104.

Endalew, A. M., Hertog, M., Gebrehiwot, M. G., Baelmans, M., Ramon, H., Nicolaï, B M., Verboven, P., 2009. Modelling airflow within model plant canopies using an integrated approach. Comput. Electron. Agric. 66, 9–24.

Endalew, A.M., Debaer, C., Rutten, N., Vercammen, J., Delele, M. A., Ramon, H. Nicolaï, B.M., Verboven, P., 2010. A new integrated CFD modelling approach towards air assisted orchard spraying. Part I. Model development and effect of wind speed and direction on sprayer airflow. Comput. Electron. Agric. 71, 128–136.

Endalew, A.M., Debaer, C., Rutten, N., Vercammen, J., Delele, M.A., Ramon, H., Nicolaï, B.M., Verboven, P., 2010b. A new integrated CFD modelling approach towards air assisted orchard spraying. Part II. Validation for different sprayer types. Comput.

Electron. Agric. 71, 137–147.

Farooq, M., Landers, A., 2004. Interactive effects of air, liquid and canopies on spray patterns of axial-flow sprayers. In: ASAE/CSAE Annual International Meeting, Ottawa, Ontario, 1-4 August.

Finnigan, J., 2000. Turbulence in plant canopies. Annu. Rev. Fluid Mech. 32, 519–571.

Finnigan, J.J., Shaw, R.H., Patton, E.G., 2009. Turbulence structure above a vegetation canopy. J. Fluid Mech. 637, 387–424.

Fornasiero, D., Mori, N., Tirello, P., Pozzebon, A., Duso, C., Tescari, E., Bradascio, R., Otto, S., 2017. Effect of spray drift reduction techniques on pests and predatory mites in orchards and vineyards. Crop Prot. 98, 283–292.

Fox, R. D., Derksen, R. C., Zhu, H., Brazee, R. D., Svensson, S. A., 2008. A history of air-blast sprayer development and future prospects. Trans. ASABE. 51, 405–410.

Ganesh, D., 2018. A review on pesticide and fertilizer used by the farmers and input dealers. J. Biofertil. Biopestic. 1, 1–2.

Garcerá, C., Moltó, E., Chueca, P., 2017. Spray pesticide applications in Mediterranean citrus orchards: Canopy deposition and off-target losses. Sci. Total Environ. 599, 1344–1362.

García-Ramos, F. J., Vidal, M., Boné, A., Malón, H., Aguirre, J., 2012. Analysis of the air flow generated by an air-assisted sprayer equipped with two axial fans using a 3D sonic anemometer. Sensors. 12, 7598-7613.

García-Ramos, F. J., Serreta, A., Boné, A., Vidal, M. 2018. Applicability of a 3D Laser Scanner for Characterizing the Spray Distribution Pattern of an Air-Assisted Sprayer. J. Sensors. 2018, 1-7.

Georgiadis, T., Dalpane, E., Rossi, F., Nerozzi, F., 1995. Orchard atmosphere physical exchanges: modelling the canopy aerodynamics. IV International Symposium on Computer Modelling in Fruit Research and Orchard Management, Avignon, 4-8 September.

Ghosh, S., Hunt, C.R., 1998. Spray jets in a cross-flow. J. Fluid Mecha 365, 109-136.

Gil, Y., Sinfort, C. 2005. Emission of pesticides to the air during sprayer application: A bibliographic review. Atmos. Environ. 39, 5183-5193.

Gil, E., Llop, J., Gallart, M., Valera, M., Llorens, J. 2015. Design and evaluation of a manual device for air flow rate adjustment in spray application in vineyards. 13th Workshop on Spray Application Techniques in Fruit Growing (Suprofruit), Lindau, 15-18 July.

Grella, M., Gil Moya, E., Balsari, P., Marucco, P., Gallart, M., 2017. Advances in developing a new test method to assess spray drift potential from air blast sprayers. Span. J. Agric. Res. 15, 1–16.

Grella, M., Marucco, P., Balsari, P., 2019. Toward a new method to classify the airblast sprayers according to their potential drift reduction: comparison of direct and new indirect measurement methods. Pest Manag. Sci. (accepted). https://doi.org/10.1002/ps.5354

Gu, J., Zhu, H., Ding, W. 2012. Unimpeded air velocity profiles of an air-assisted five-port sprayer. Trans. ASABE. 55(5), 1659-1666.

Hołownicki, R., Doruchowski, G., Świechowski, W., Godyń, A., Konopacki, P.J., 2017. Variable air assistance system for orchard sprayers; concept, design and preliminary testing. Biosyst. Eng. 163, 134–149.

Hong, S. W., Zhao, L., Zhu, H., 2018. CFD simulation of airflow inside tree canopies discharged from air-assisted sprayers. Comput. Electron. Agr. 149, 121-132.

ISO, 2000. ISO/FDIS 9898. Equipment for crop protection. Test methods for air-assisted sprayers for bush and trees. International Standards Organization, Geneva (Switzerland).

ISO, 2005. ISO/FDIS 22866. Equipment for crop protection. Methods for the field measurement of spray drift. International Standards Organization, Geneva (Switzerland).

Kasner, E.J., Fenske, R.A., Hoheisel, G.A., Galvin, K., Blanco, M.N., Seto, E.Y., Yost,

M.G., 2018. Spray drift from a conventional axial fan air blast sprayer in a modern orchard work environment. Ann. Work Expo. Health. 62, 1134–1146.

Landers. A.J., 2008. Improving spraying efficiency. In: National wine and grape industry centre, NWGIC Workshop. Available at

www.nysaes.cornell.edu/ent/faculty/landers/pestapp [accessed 15 September 2018].

Landers, A. Farooq, M., 2004. Factors influencing air and pesticide penetration into grapevine canopies. Asp. Appl. Biol. 71, 343-348

Larbi, P.A., Salyani, M., 2012a. Model to predict spray deposition in citrus airblast sprayer applications; part 1. Spray dispersion. Trans. ASABE, 55(1), 29–39.

Larbi, P.A., Salyani, M., 2012b. Model to predict spray deposition in citrus airblast sprayer applications; part 2. Spray deposition. Trans. ASABE. 55, 41–48

Li, L., He, X., Song, J., Liu, Y., Zeng, A., 2018. Airflow decision-making model to match the canopy characteristics. ASABE Annual International Meeting, Detroit, 29-1 August.

Longlong, L., Xiongkui, H., Jianli, S., Xionan, W., Xiaoming, J., Chaohui, L. 2017. Design and experiment of automatic profiling orchard sprayer based on variable air volume and flow rate. Trans. CSAE. 33, 70-76.

López-Lozano, R., Baret, F., de Cortázar-Atauri, I. G., Bertrand, N., Casterad, M. A., 2009. Optimal geometric configuration and algorithms for LAI indirect estimates under row canopies: The case of vineyards. Agr. Forest Meteorol. 149, 1307-1316.

Mamane, A., Raherison, C., Tessier, J.F., Baldi, I., Bouvier, G., 2015. Environmental exposure to pesticides and respiratory health. Eur. Respir. Rev. 24, 462-473.

Miranda, A., Rodríguez, A., Gil, E., Agüera, J., Gil, J.A., 2015. Influence of liquid volume and airflow rates on spray application quality and homogeneity in super intensive olive tree canopies. Sci. Total Environ. 537, 250–259.

Miranda, A., Rodríguez, A., Cuenca, A., González, E. J., Blanco, G. L., Gil, J. A., 2017. Improving plant protection product applications in traditional and intensive olive orchards through the development of new prototype air-assisted sprayers. Crop Prot. 94, 44-58.

Miranda, A., Marucco, P., González, E.J., Gil, E., Grella, M., Balsari, P., 2018. Developing strategies to reduce spray drift in pneumatic spraying in vineyards: Assessment of the parameters affecting droplet size in pneumatic spraying. Sci. Total Environ. 616, 805-815.

Moltó, E., Garcerá, C., Chueca, P., 2006. Manejo de turboatomizadores para el cultivo de cítricos. Vida Rural. 237, 56-62.

Ochoa, V., Maestroni, B., 2018. Pesticides in water, soil, and sediments, in: Maestroni, B., Cannavan, A., (Eds), Integrated Analytical Approaches for Pesticide Management. Academic Press, Vienna, pp. 133–147

Panneton, B., Lacasse, B., Piché, M., 2005a. Effect of air-jet configuration on spray coverage in vineyards. Biosyst. Eng. 90, 173-184.

Panneton, B., Lacasse, B., Thériault, R., 2005b. Penetration of spray in apple trees as a function of airspeed, airflow, and power for tower sprayers. Can. Biosyst. Eng. 47, 13-20.

Pascuzzi, S., 2013. The effects of the forward speed and air volume of an air-assisted sprayer on spray deposition in tendone trained vineyards. J. Agric. Eng. 44, 1-18.

Pergher, G., Gubiani, R., 1995. The effect of spray application rate and airflow rate on foliar deposition in a hedgerow vineyard. J. Agric. Eng. Res. 61, 205-216.

Pergher, G., 2006. The effect of airflow rate and forward speed on spray deposition from a vineyard sprayer. J. Agric. Eng. 1, 17-23.

Pergher, G., Petris, R., 2008. The effect of air flow rate on spray deposition in a guyot trained vineyard. Agricultural Engineering International: the CIGR Ejournal X (May), Manuscript ALNARP 08 010

Pezzi, F., Rondelli, V., 2000. The performance of an air-assisted sprayer operating in vines. J. Agric. Eng. Res. 76, 331–340.

Reichard, D.L., Retzer, H.J., Liljedahl, L.A., Hall, F.R., 1977. Spray droplet size distributions delivered by air blast orchard sprayers. Trans. ASAE. 20, 232-237.

Reichard, D.L., Fox, R.D., Brazee, R.D., Hall, F.R., 1979. Air velocities delivered by orchard air sprayers. Trans. ASAE. 22, 69-74.

Reichard, D.L., Zhu, H., Fox, R.D., Brazee, R.D., 1992. Wind tunnel evaluation of a computer program to model spray drift. Trans. ASAE. 35, 755–758.

Salcedo, R., Garcerá, C., Granell, R., Moltó, E., Chueca, P., 2015. Description of the airflow produced by an air-assisted sprayer during pesticide applications to citrus. Span. J. Agric. Res. 13, 2–8.

Svensson, S.A., Brazee, R.D., Fox, R.D., Williams, K.A., 2003. Air jet velocities in and beyond apple trees from a two-fan crossflow sprayer. Tran. ASAE. 46, 611–621.

Świechowski, W., Doruchowski, G., Holownicki, R., Godyn, A., 2004. Penetration of air within the apple tree canopy as affected by the air jet characteristics and travel velocity of the sprayer. Electron. J. Pol. Agric. Univ 7 (2). Available at http://www.ejpau.media.pl/volume7/issue2/engineering/art-03.html [accessed 15 September 2018].

TOPPS-Prowadis Project, 2014. Best management practices to reduce spray drift. Available at http://www.topps-life.org/ [accessed 15 September 2018].

Triloff, P. 2011. Verlustreduzierter Pflanzenschutz im Baumobstbau. Abdriftminimierung und Effizienzsteigerung durch baumformabhängige Dosierung und optimierte Luftführung. Dissertation Universität Hohenheim, Institut für Agrartechnik, Verlag Grauer, Beuren, Stuttgart., 351.

Triloff, P. 2015. Results of measuring the air distribution of sprayers for 3D-crops and parameters for evaluating and comparing fan types. 13th Workshop on Spray Application Techniques in Fruit Growing (Suprofruit), Lindau, 15-18 July.

Triloff, P., 2016. Results and conclusions from five years measuring and adjusting air distribution of brand-new sprayers for 3D Crops. 6th European workshop on standard procedure for the inspection of sprayers in Europe (SPISE), Castelldefels, 13-15 September.

Triloff, P., 2018. A case study-canopy adapted dosing and spray application in 3D crops. Dose Expression Workshop. Association of Applied Biologist. Castelldefels, 6-7 November.

Van de Zande, J. C., Schlepers, M., Hofstee, J. W., Michielsen, J. G. P., Wenneker, M.,2017. Characterization of the air flow and the liquid distribution of orchard sprayers. 14th Workshop on Spray Application Techniques in Fruit Growing (Suprofruit), Hasselt, 10-12 July.

Walklate, P.J., Weiner, K.L., Parkin, C.S., 1996. Analysis of and experiment measurements made on a moving air-assisted sprayer with two-dimensional air-jets penetrating a uniform crop canopy. J. Agric. Eng. Res. 63, 365–378.

Walklate, P. J., Richardson, G. M., 2000. Relationship between orchard tree crop structure and performance characteristics of an axial fan sprayer. Asp. Appl. Biol. 57, 285-292.

Wei, Q., Sanqin, Z., Weimin, D., Chengda, S., Jiang, L., Yinian, L., Jiabing, G., 2016. Effects of fan speed on spray deposition and drift for targeting air-assisted sprayer in pear orchard. Int. J. Agric. & Biol. Eng. 9, 53-62.

Zhai, C., Zhao, C., Wang, N. Long, J., Wang, X., Weckler, P. R., Zhang, N., 2018. Research progress on precision control methods of air-assisted spraying in orchards. Trans. CSAE. 34, 1-15.

Zhu, H., Reichard, D.L., Fox, R.D., Brazee, R.D., Ozkan, H.E., 1994. Simulation of drift of discrete sizes of water droplets from field sprayers. Trans. ASAE. 37, 1401-1407.

Figure captions

Figure 1. Schematic of the artificial canopies with dimensions.

Figure 2. Axial fan sprayer between the artificial canopies during the trials.

Figure 3. Schematic of the static airflow test: plan view of the layout of the measuring points (i) and elevation view of the fan position with respect to the canopies (ii).

Figure 4. Plan view of the layout of the measuring points during the dynamic field tests.

Figure 5. Zone divisions characterizing the dynamic field test.

Figure 6. Total mean velocities magnitudes and standard deviation between repetitions at both sides of the fan before and after the canopies during the static assay in the plane of the air outlet of the fan (z = 0.6 m).

Figure 7. Air velocity vectors in the XY-plane during the static assay. Distance in meters (m).

Figure 8. Air velocity vectors in the ZY-plane during the static assay. Vectors were showed post by post, considering the presence (or none) of an obstacle behind the post. Distance in meters (m).

Figure 9. Total mean turbulence intensity and standard deviation between repetitions on both sides of the fan before and after the canopies during the static assay.

Figure 10. Total mean velocity magnitudes and standard deviation between repetitions on both sides of the fan before and after the canopies in the dynamic assay during (i) the first third on entering, (ii) the middle third, and (iii) the last third before leaving the canopies.

Figure 11. Air velocity vectors in the XY-plane in the dynamic assay during (i) the first third on entering, (ii) the middle third, and (iii) the last third before leaving the canopies. The vortices were marked.

Figure 12. Air velocity vectors in the ZY-plane in the dynamic assay during (i) the first one-third of the height of the canopy on entering, (ii) the middle one-third of the height of the canopy and (iii) the final one-third of the height of the canopy before leaving the canopies. Distance is in meters.

Figure 13. Total mean turbulence intensities and standard deviation between repetitions in the dynamic assay in (i) the first third of the height of the canopy on entering, (ii) the middle third of the height of the canopy and (iii) the last third of the height of the canopy before leaving the canopies.

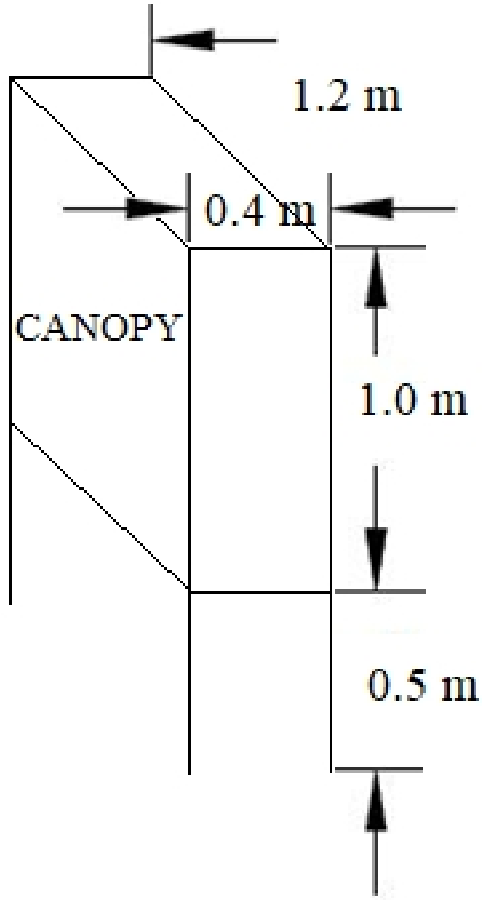
1.2 m
0.4 m
CANOPY
1.0 m
0.5 m

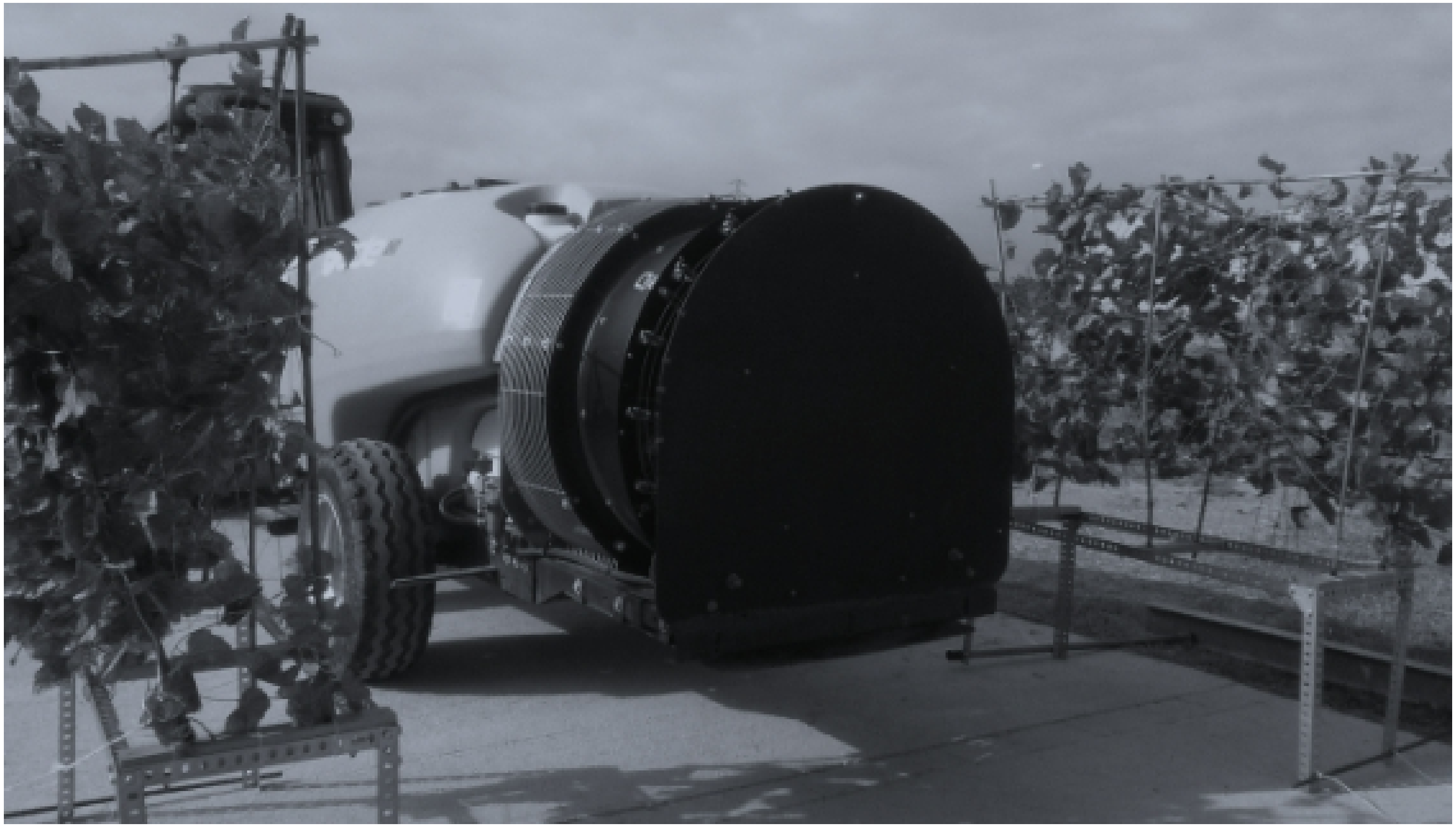

i)

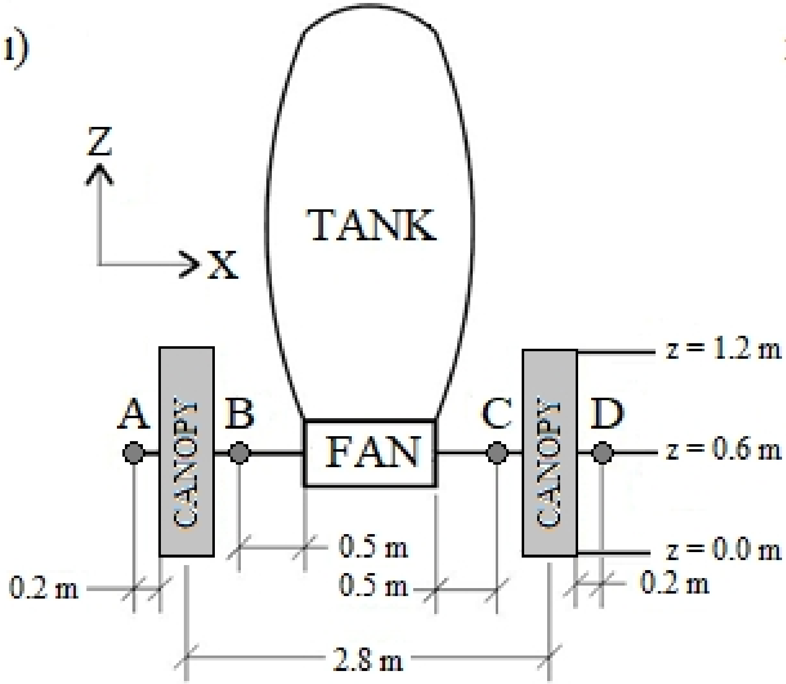

Z
X
TANK
FAN
A
CANOPY
B
C
CANOPY
D
z = 1.2 m
z = 0.6 m
z = 0.0 m
0.5 m
0.5 m
0.2 m
0.2 m
2.8 m

ii)

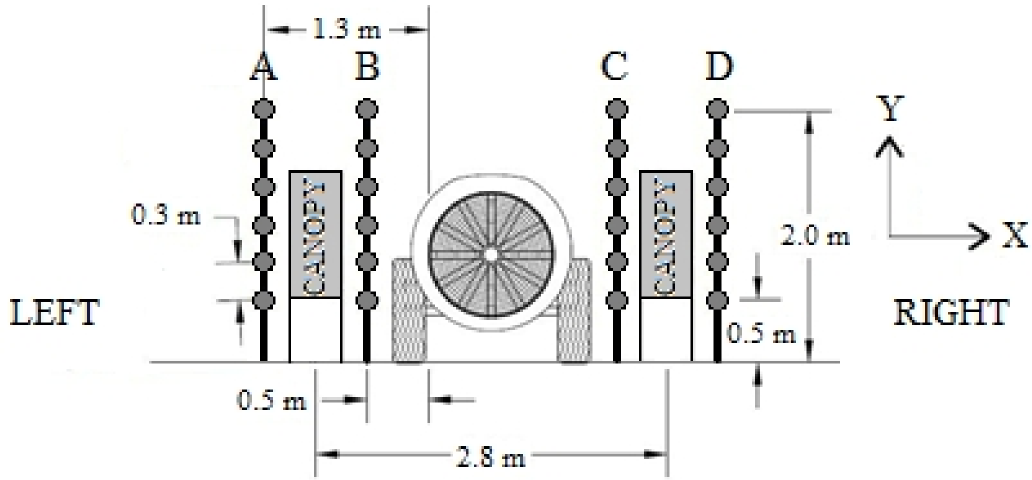

1.3 m
A
B
C
D
Y
X
0.3 m
CANOPY
CANOPY
2.0 m
LEFT
RIGHT
0.5 m
0.5 m
2.8 m

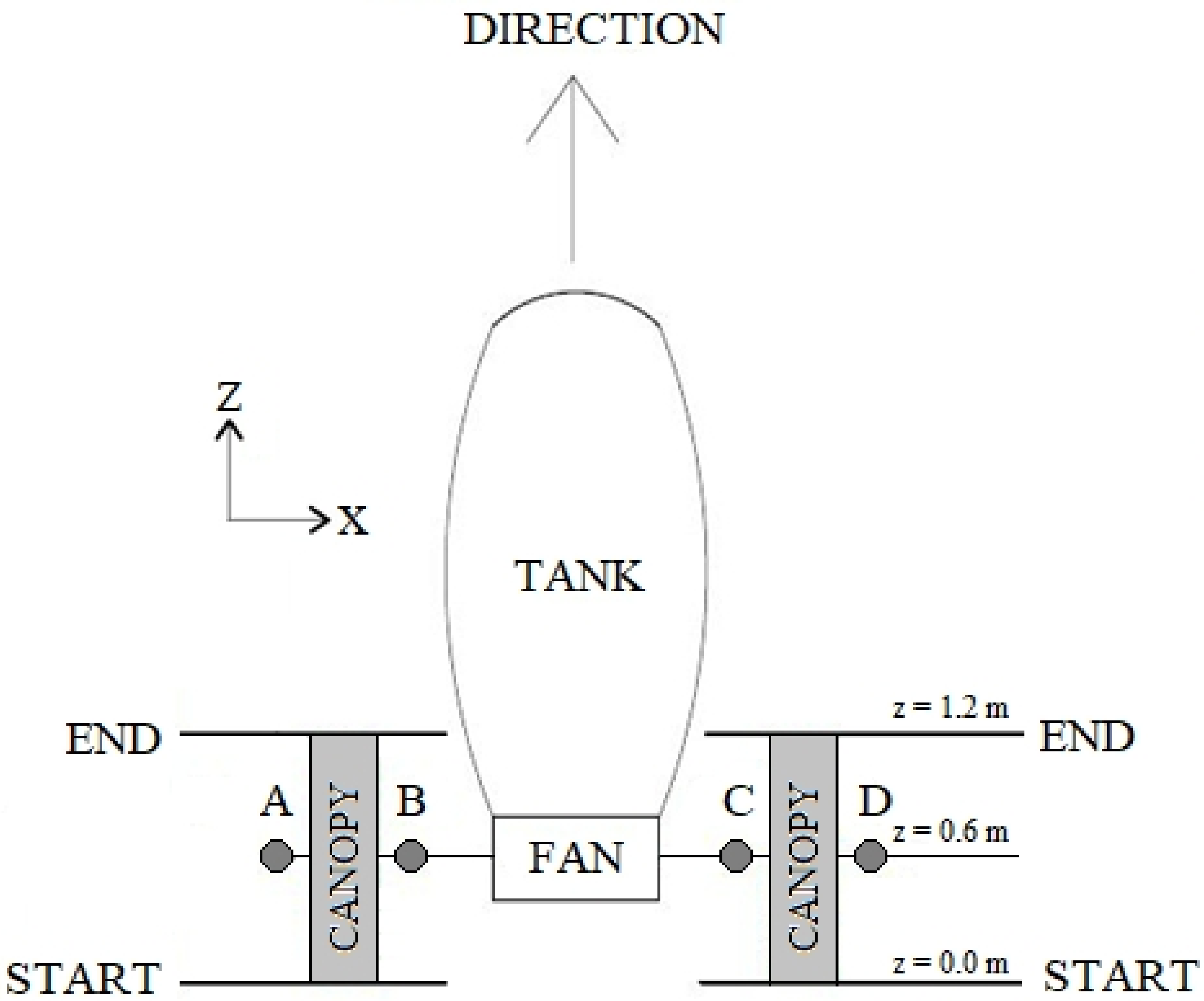
DIRECTION
Z
X
TANK
END
START
A
B
C
D
CANOPY
CANOPY
FAN
z = 1.2 m
z = 0.6 m
z = 0.0 m
END
START

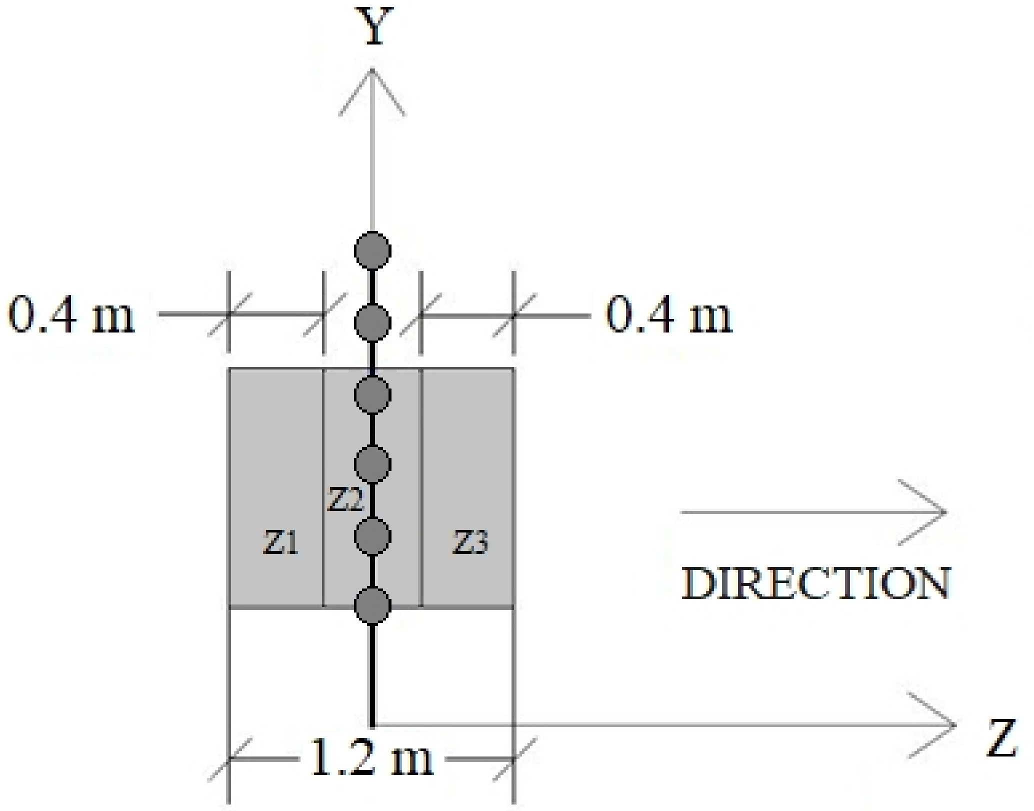
Y
0.4 m
0.4 m
Z2
Z1
Z3
DIRECTION
Z
1.2 m

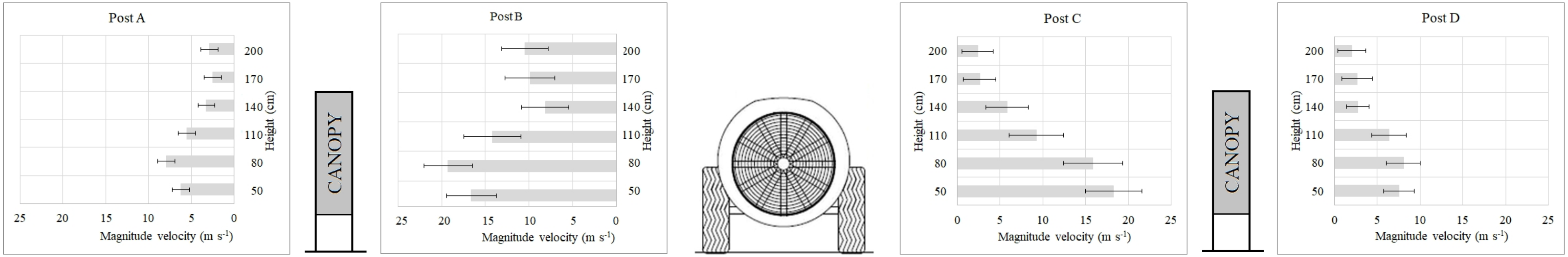
Post A
Post B
Post C
Post D
CANOPY
CANOPY
Height (cm)
200
170
140
110
80
50
25
20
15
10
5
0
Magnitude velocity (m s-1)

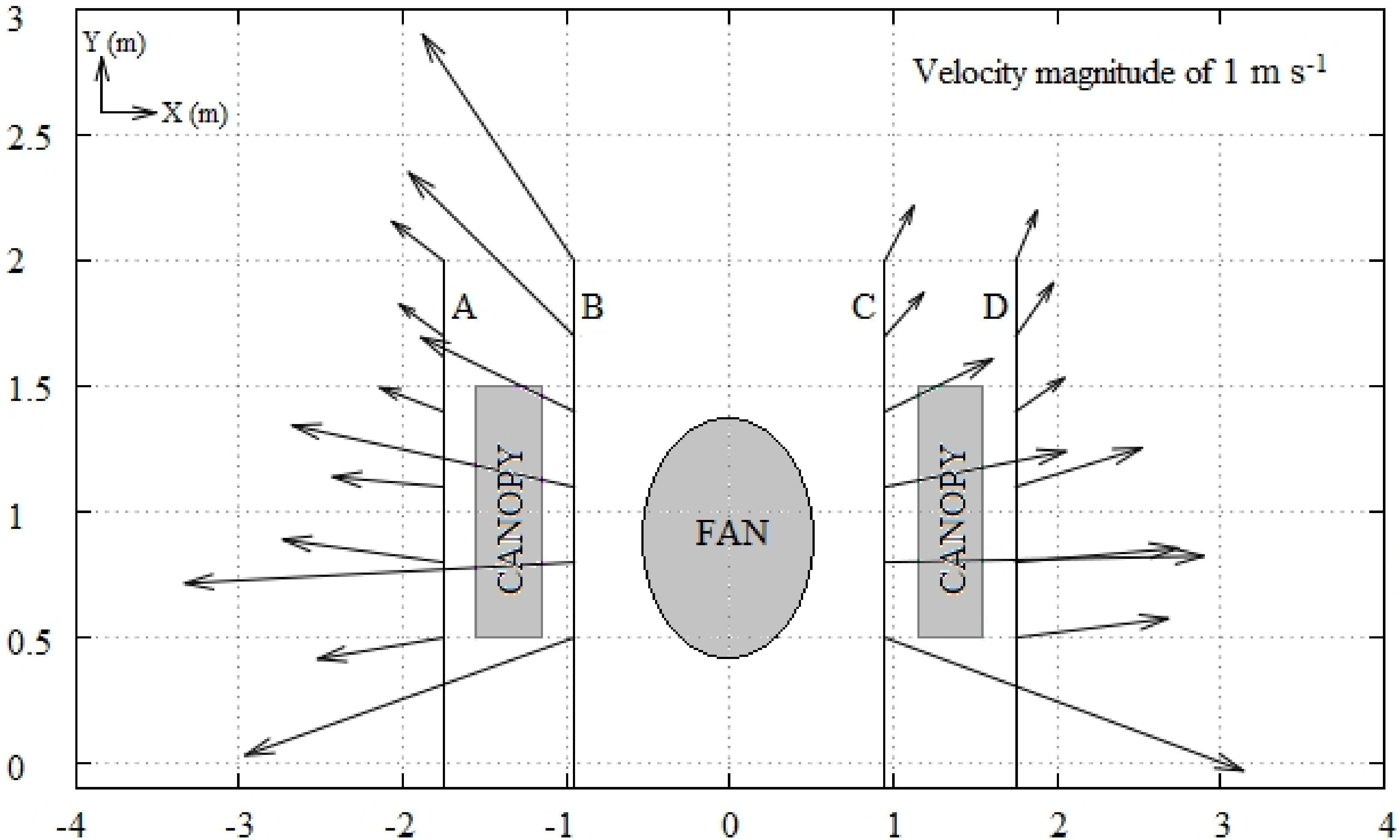

Y (m)
X (m)
Velocity magnitude of 1 m s-1
A
B
C
D
CANOPY
FAN
CANOPY
3
2.5
2
1.5
1
0.5
0
-4
-3
-2
-1
0
1
2
3
4

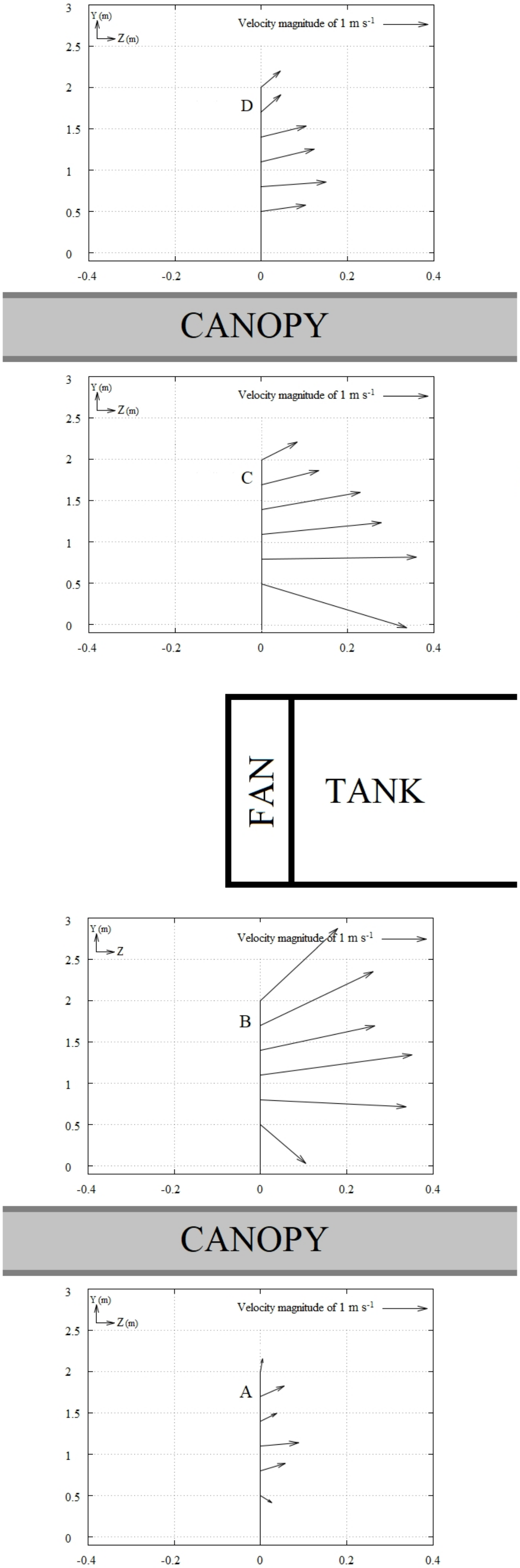
Velocity magnitude of 1 m s-1
Y (m)
Z (m)
D
CANOPY
C
FAN
TANK
B
A
-0.4
-0.2
0
0.2
0.4
0.5
1
1.5
2
2.5
3

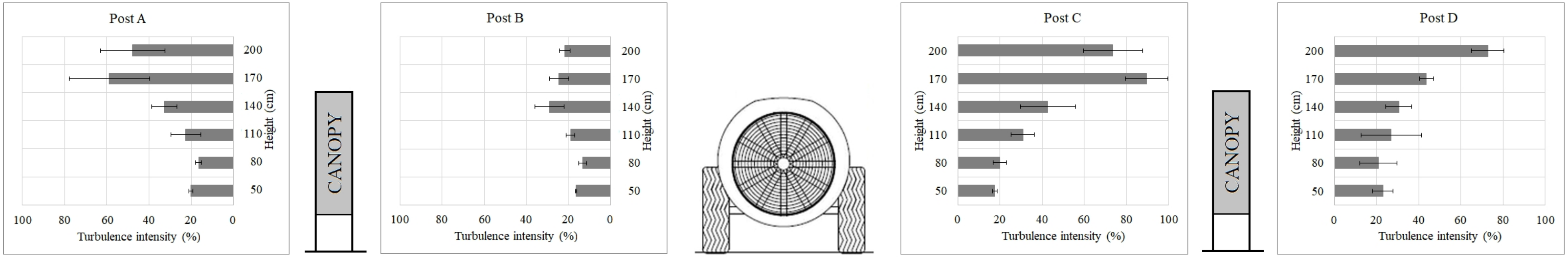

Post A
200
170
140
110
80
50
Height (cm)
100 80 60 40 20 0
Turbulence intensity (%)
CANOPY
Post B
200
170
140
110
80
50
Height (cm)
100 80 60 40 20 0
Turbulence intensity (%)
Post C
Height (cm)
200
170
140
110
80
50
0 20 40 60 80 100
Turbulence intensity (%)
CANOPY
Post D
Height (cm)
200
170
140
110
80
50
0 20 40 60 80 100
Turbulence intensity (%)

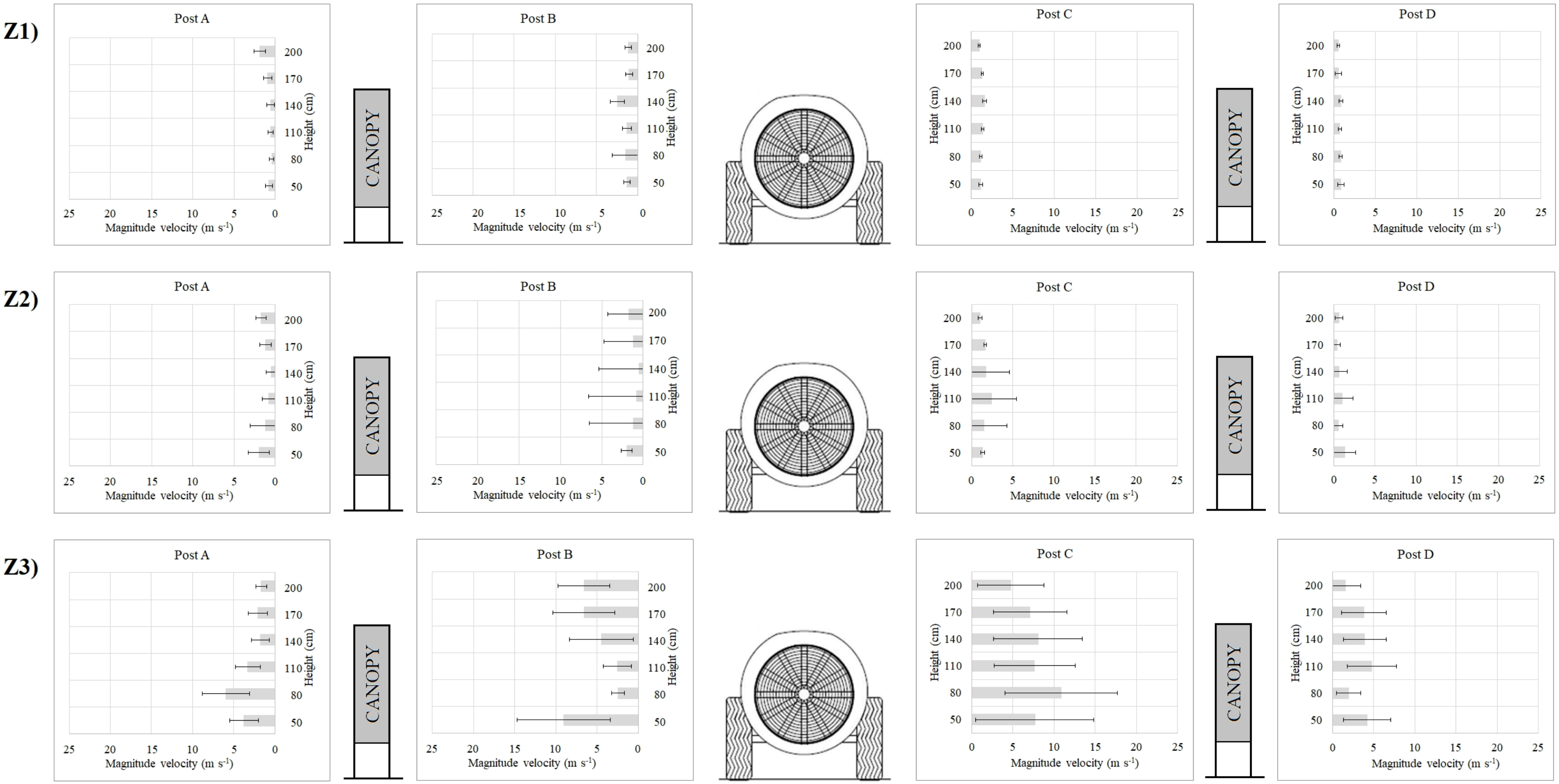
Z1)
Z2)
Z3)
Post A
Post B
Post C
Post D
CANOPY
Height (cm)
Magnitude velocity (m s-1)
200
170
140
110
80
50
25
20
15
10
5
0

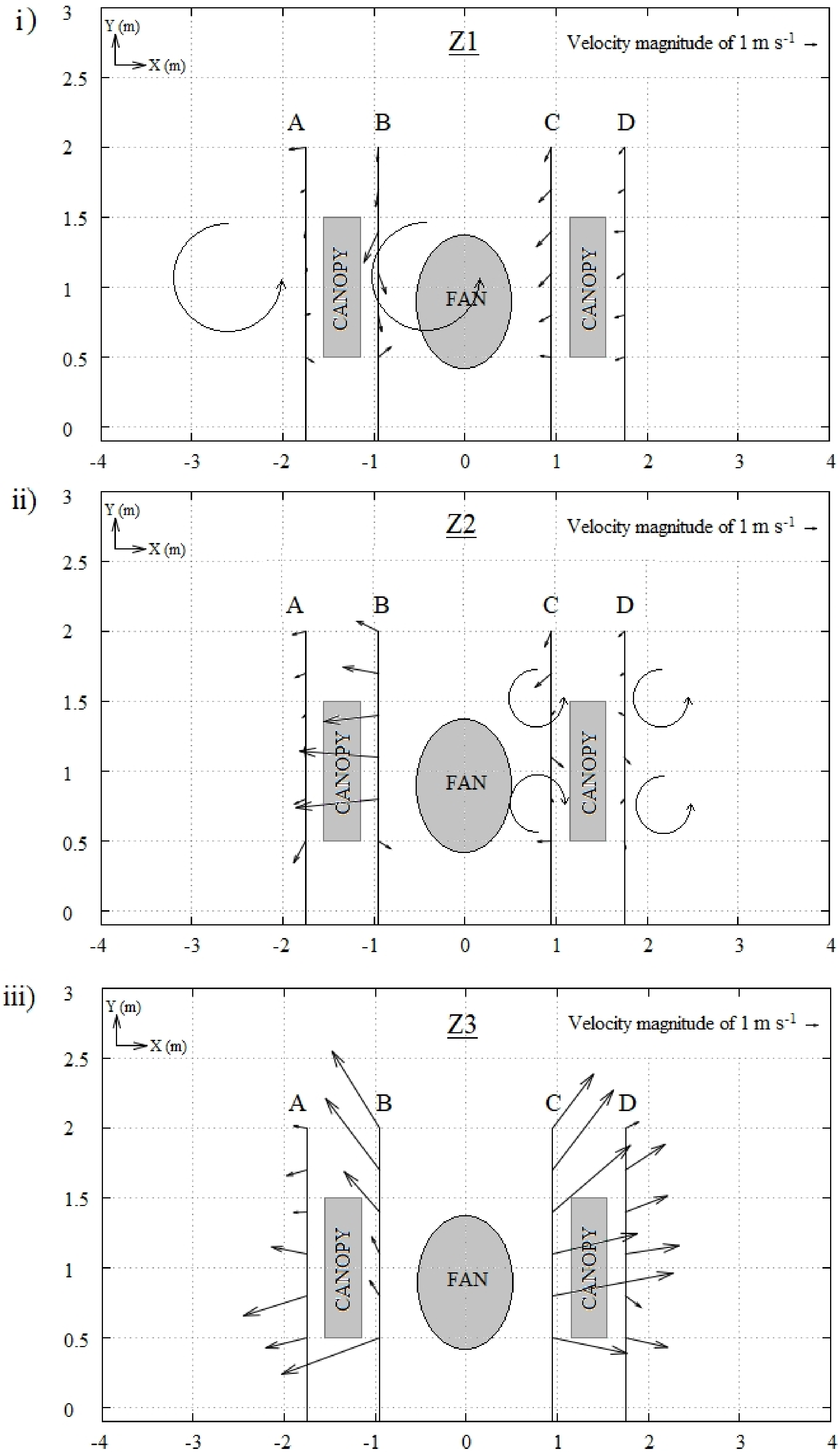

i)
Y (m)
X (m)
Z1
Velocity magnitude of 1 m s-1
A
B
C
D
CANOPY
FAN
CANOPY
3
2.5
2
1.5
1
0.5
0
-4
-3
-2
-1
0
1
2
3
4
ii)
Y (m)
X (m)
Z2
Velocity magnitude of 1 m s-1
A
B
C
D
CANOPY
FAN
CANOPY
3
2.5
2
1.5
1
0.5
0
-4
-3
-2
-1
0
1
2
3
4
iii)
Y (m)
X (m)
Z3
Velocity magnitude of 1 m s-1
A
B
C
D
CANOPY
FAN
CANOPY
3
2.5
2
1.5
1
0.5
0
-4
-3
-2
-1
0
1
2
3
4

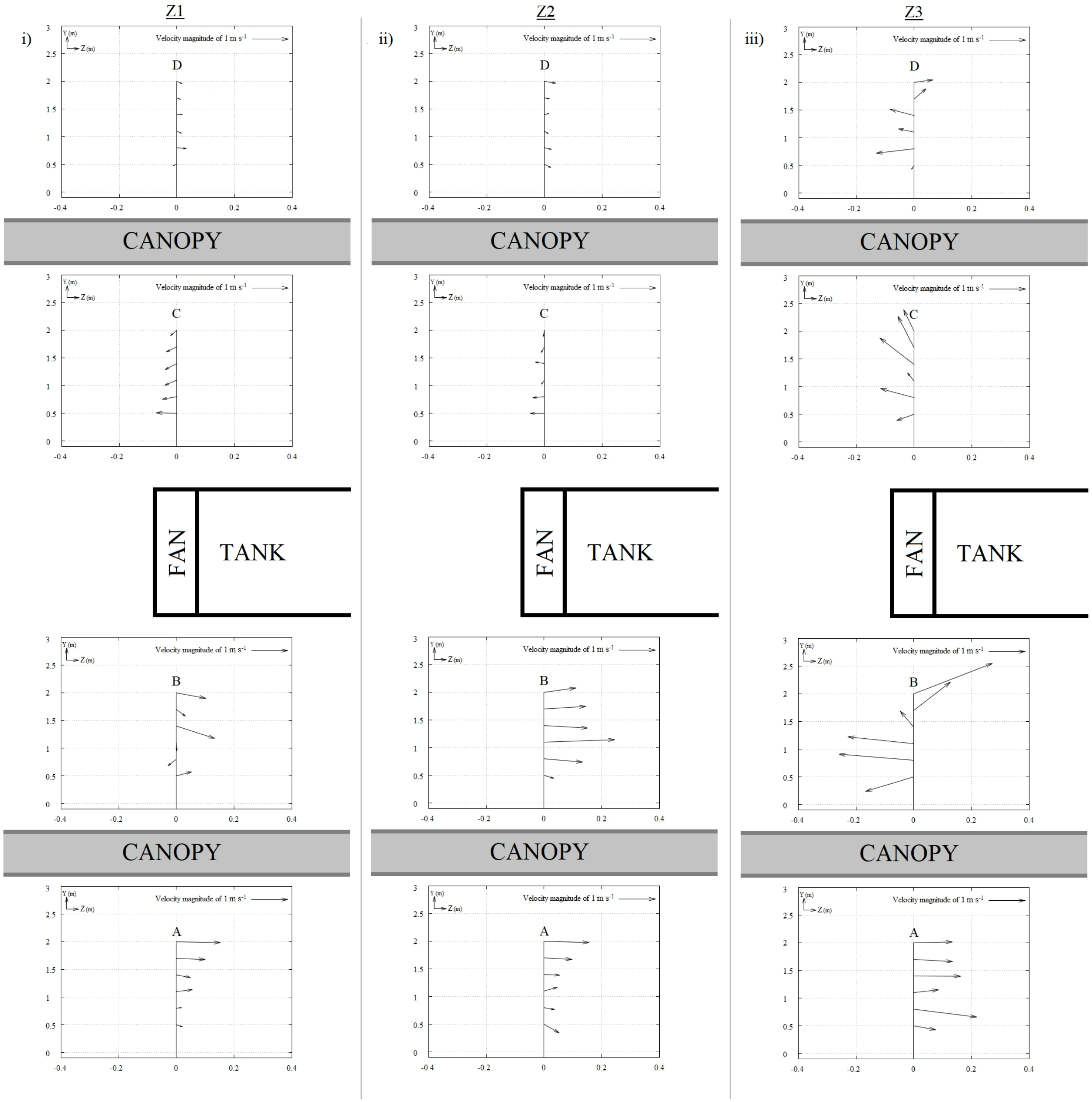
Z1
Z2
Z3
i)
ii)
iii)
Velocity magnitude of 1 m s-1
Y (m)
Z (m)
D
C
B
A
CANOPY
FAN
TANK

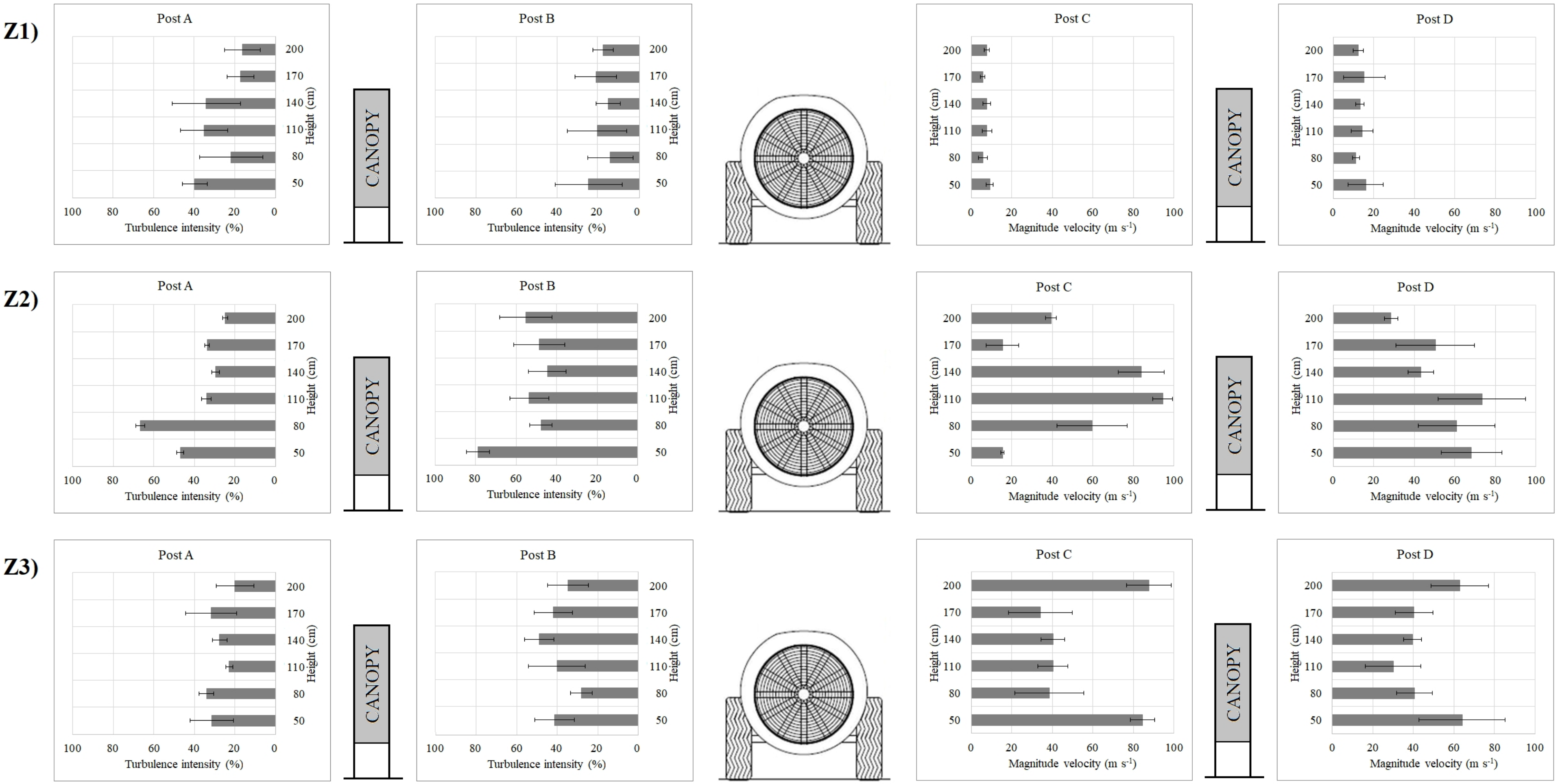
Z1)
Z2)
Z3)
Post A
Post B
Post C
Post D
Turbulence intensity (%)
Magnitude velocity (m s-1)
Height (cm)
200
170
140
110
80
50
0
20
40
60
80
100
CANOPY